however its main function is to facilitate merozoite invasion. This is further supported by our data obtained by quantitative PCR, which illustrate that the Pf332 gene is activated at a later time point during the erythrocytic life cycle than the *var*-genes. Even though the DBL-domain of Pf332 is homologous to RBC invasion-related proteins such as EBA-175 it clearly differs from these microneme- and rhoptry-related molecules regarding the time of transcription initiation (starts at around 38 h p.i. for these proteins, PlasmoDB). Hence, Pf332 displays a distinct expression profile, clearly distinguishing it from other *P. falciparum* surface molecules pointing at a unique function of this molecule in the parasite life cycle. Pf332 presents a novel type of invasion-related molecule facilitating and supporting the invasion of future merozoites, clearly different from other cytoadhesion-related proteins such as PfEMP1 or merozoite invasion ligands (e.g. MSPs).

Despite the major interest in Pf332, its characterization has been hampered by the fact that many of the α-Pf332 antibodies are cross-reactive with other molecules, e.g. the Pf155/RESA also containing regular repeats of glutamic acid [33]. Western blot analysis of our antibodies raised against the DBL/nDBL-region of the newly discovered exon I of Pf332 has revealed that these antibodies are specifically reacting with the Pf332. They do not recognize or cross-react with any other parasite antigens neither in Western blot nor immunoflurescence assays carried out on merozoites (Fig 3C, 4E and data not shown) supporting the conclusion that the reduction of invasion efficiency of the α-Pf332-DBL/nDBL antibody is specific. We could show that both recombinant protein and antibodies to the DBL-domain of Pf332 reduce parasite invasion, while antibodies towards the PfEMP1 (α-DBL1-domain) did not (Fig. 6 and data not shown). Comparing the effect of our α-Pf332 antibodies with antibodies known to target the process of invasion [6,7], a similar inhibitory effect is observed, indicating that Pf332 might harbour a function during the merozoite invasion process.

In conclusion, we have identified a molecule with a conserved RBC-binding DBL-domain that plays an important role in invasion of the *P. falciparum* parasite. The protein is apparently essential for the efficient proliferation of all *P. falciparum* parasites. This discovery can have important implications in malaria vaccine development as well as in designing new drugs to block parasite invasion.

MATERIALS AND METHODS

Bioinformatic analysis of the upstream sequence of the Pf332 gene in the 3D7 genome

Analysis of the 3D7 parasite genome for sequences containing RBC-binding motifs led to the identification of a hypothetical gene (PF11_0506) located 281 bp upstream of the gene Pf332, which potentially encodes a RBC-binding domain. PF11_0506 has one ORF with a size of 1710 bp. The putative sequence of this polypeptide was aligned with sequences of several EBL-family proteins. The secondary structure and the cellular locations were analysed with the Macvector program (GCG, UK).

Gene transcription and analysis

From total RNA purified with TRIZol®[34] first strand cDNA was synthesized (GeneAmp RNA PCR Kit, Applied Biosystems, USA) and further amplified with the primers UP3 (TAG TAC CAG GAG TAT TAA CA) and UP4 (TTC CGT GTA TCT TCT TCT TC) (Fig. 1). Northernblot was carried out with two anti-sense digitonin-labelled RNA probes as described [4]. The RNA probes were generated from two plasmids; plasmid 1 containing a sequence amplified with primers UP1 (ATG TCT AAT ATA AAT AAC AAA GAC TC) and UP2 (AGA ATT CAT CAC AAC TCT CAT); plasmid 2 with a fragment amplified from cDNA with primer UP3 and UP4 (Fig. 1).

Gene amplification and sequence analysis

To investigate the polymorphism of exon I, gDNA was purified (from FCR3S1.2, 3D7AH1, NF54CSA, FCR3CSA, TM284, R29, Dd2, K1, F32, FCB-3 and the Ugandan isolate UAS22, standard methods) and PCR-amplification was carried out with primers UP1 (ATG TCT AAT ATA AAT AAC AAA GAC TC) and UP5 (TAT TAC CTT ATA TAC CAA GAC C) (Fig. 1). Products were cloned into the pCRII vector (Invitrogen USA) for sequencing.

Real-time quantitative PCR analysis of Pf332 transcription

RNA was harvested at 4 h p.i. intervals (RNeasy® Mini Kit, Qiagen, Valencia, CA) and reverse transcriped (SuperScript III RNase H reverse transcriptase, Invitrogen). For real-time quantitative PCR reactions to monitor the relative expression of Pf332 to the endogenous control *seryl-tRNA synthetase* we employed an MGB-probe approach. Primers and probes were for Pf332: AAG AAG ATG TGG GAT GTG TTC CA, CAT TTT CAT TAT CCA ACC TTT CCA T and 6-FAM-CTA GGAG ACA GAA TTT GA-MGB and for *seryl-tRNA synthetase*: TAT CAT CTC AAC AGG TAT CTA CAT CTC CTA, TTT GAG AGT TAC ATG TGG TAT CAT CTT TT and 6-FAM-AAA GAT ATC ATC ACA GGC AGA T-MGB. Amplification reactions were done in quadruplicates in MicroAmp 96 well plates in 20 µl, containing TaqMan buffer with UNG (Applied Biosystems), 900 nM of each forward and reverse primer, 200 nM of each probe and 2 ng of template. 45 cycles (95°C for 15 sec and 60°C for 1 min) were performed in an ABI sequence detector 7500 (Applied Biosystems). The detection threshold was set above the mean baseline value for the first 6-15 cycles. Amplification efficiencies were verified by performing amplifications using different concentrations of cDNA for the target (Pf332) and reference (*seryl-tRNA synthetase*) and were sufficiently close to obviate the need for a correction factor. Results were analyzed by the Relative Standard Curve Method where a normalized target value was achieved by dividing the $\bar{x}_{\text{target}}$ with the $\bar{x}_{\text{reference}}$ for each clone/strain and time point. The standard deviation of the quotient was calculated according to the User Bulletin 2 (Applied Biosystems, http://www.appliedbiosystems.com). Results were visualized as $\log_2$ transformed values plotted using SigmaPlot 9.0 (Systat Software Inc.). Statistically significant strain differences in Pf332 transcription were determined for each time point performing group comparisons with One Way ANOVA and the Tukey test.

Generation of recombinant Pf332-DBL- and nDBL-fusionproteins and binding to human RBC

GST- or his-fusion proteins were generated by cloning the ORF of the DBL- and nDBL-domain into the pGEX-4T-1- (Amersham Biosciences, Sweden, primer: Pf332-DBL: forward: *GGA TCC* AGC AAC ATC AAC AAC AAG GA and reverse: *CTC GAG* GTA CTT CTT CTC GAA CAC C; Pf332-nDBL: forward: *GGA TCC* GCT AAT GAT AAT AAA TCA AAA CA and reverse: *CTC GAG* TAT TTC CTG CAT TCA TTC C) or pQE60-vector (Qiagen) (primer F-DBL: *GCA TGC* GAA GCA ACA TCA ACA ACA AGG, R-DBL: *GGA TCC* GTA CTT CTT CTC GAA CAC C) and recombinant proteins were expressed as described [35].

Recombinant protein (200 pmol) was incubated with 5 µl of washed RBC in RPMI for 2.5 h at 4°C, washed and bound protein was visualized by Westernblot (α-GST mAb, dilution 1:5000, Sigma; α-mouse mAb-ALP, dilution 1:10000, Sigma). In

addition, RBCs were treated with neuraminidase (0.2 U in PBS for 1 h at 37°C), heparitinase (0.5 U in 50 mM Tris for 1 h at 37°C) or trypsin (100 μg/ml in PBS for 1 h at 37°C) in a 20 μl scale before the binding assays.

Surface-expression of the Pf332-DBL- and Pf332-nDBL-domain on CHO-cells and binding to human RBC

The Pf332-DBL- (optimized for expression in mammalian cells, GeneArt, Germany) and Pf332-nDBL-domain were cloned into the pDisplay vector (Invitrogen). Transfection of CHO-cells was performed with the FuGENE 6 transfection reagent (Roche Applied Science, Switzerland) and expression of the domains on the cell surface was confirmed by immunofluorescence 48 h later (α-HA-antibody, Invitrogen; Alexa-labelled-α-mouse-antibody, Molecular probe, USA).

For detection of RBC-binding transfected CHO-cells were detached, and stained with PKH67 (green); human RBC were in parallel stained with PKH26 (red). CHO-cells were incubated with RBC at a ratio of 1:5 for 1 h at RT and the rosette formation was afterwards analysed by fluorescence microscopy.

Generation of specific antibodies against the region encoded by exon I of Pf332

The region encoded by exon I of Pf332 (aa 1–533) was cloned into the Semliki forest virus vector SFV3.spider (primer: 332-F-SFV (*CCC GGG* ATG TCT AAT ATA AAT AAC AAA GAC and 332-RII-SFV (*CCC GGG* ATA ATT TCC TGC ATT CAT TCC ATC) and virus particles generated as described before [36]. Rabbits (New Zeeland white) or rats were immunized (three times 5×10^8 particles/animal, once 500 μg protein/animal, respectively four times 100 μg protein/animal).

Immunodetection of Pf332 in Westernblot and immunofluorescence on fixed and live iRBC

Trophozoite iRBC were purified [37,38], lysed in SDS-loading buffer, analyzed by 6% SDS-PAGE (2×10^6 cells/lane) and subjected to various α-Pf332 sera. Visualization was performed with an α-rabbit Ig- (1:5000, Amersham) or an α-human Ig-HRP-conjugate (1:1500, Amersham).

For immunofluorescence assays, monolayers of iRBC were prepared as described before [18]. Monolayers were incubated 30 min with the α-Pf332-DBL/nDBL antibody (1:800) or pre-immune serum (1:800), washed three times in PBS, and incubated 30 min with a secondary antibody (α-rabbit-Alexa, Molecular Probes, 1:100).

For live IFA-assays, monolayers were prepared on adhesive slides (Marienfeld Glassware) according to the manufacturer's protocol. Negatively charged cells are bound to these slides based on electrostatic adhesion without additional fixation steps allowing the investigation of live late-stage iRBC. The cells were incubated with the α-Pf332-DBL antibody (1:50), pre-immune serum (1:50), α-PfEMP2 (1:50) or serum to an unrelated control protein (1:50), washed three times in PBS, and incubated with a secondary antibody (α-rat-Alexa, Molecular Probes, dilution 1:300) and counterstained with Ethidium-bromide. All incubations were carried out at room temperature in a humid chamber. Slides were analyzed with a 100×oil immersion lens in a Nikon Optiphot 2 UV microscope.

Invasion inhibition assay

IRBC of various parasite clones/strains at trophozoite stage were adjusted to a parasitemia of 1% and a hematocrit of 2.5%, mixed with the purified IgG fraction of an α-Pf332-DBL/nDBL-, α-GST- or α- AMA1/MSP1-serum [39] in final concentrations of 1, 0.5 and 0:25 mg/ml (in duplicates) and cultivated in 96-well plates until reinvasion of merozoites was completed. IRBC were stained with Acridine Orange and counted (50,000 events) by flow cytometry. Experiments were repeated three times and the effect was determined by relating the observed parasitemia in the presence of α-Pf332-DBL/nDBL- or α-AMA1/MSP1-antibodies to α-GST antibodies (negative control).

SUPPORTING INFORMATION

Figure S1 The sequence of the exon I of Pf332 is conserved among various parasite clones/strains. PCR amplification of the exon I region of the Pf332 gene from gDNA of various parasites showed a single product of 1710 bp (primer UP1 and UP5; compare Fig. 1A) from 10 different P. falciparum clones/strains and one Ugandan isolate. Enzymatic treatment of the amplified fragments with EcoR I illustrated that there was only one sequence in each amplicon. All amplified products were cloned and sequenced and only 4 mutations were identified among the 11 sequences (compare table 1).
Found at: doi:10.1371/journal.pone.0000477.s001 (0.24 MB TIF)

Figure S2 Alignment of the amino acid sequence of the EBL-family members. The sequence of Pf332 encoded by exon I shares numerous amino acid residues (highlighted with stars) that are conserved among the erythrocyte-binding proteins of different Plasmodium-species such as the sequences of the DBL-domain of the P. vivax Duffy binding protein (DBP), P. knowlesi DBP, P. cynomolgi DBP, BAEBL/EBA-140, JESEBL/EBA-181 and EBA-175 of P. falciparum
Found at: doi:10.1371/journal.pone.0000477.s002 (0.31 MB TIF)

Figure S3 Immunoblot analysis of the molecule Pf332. Antibodies towards the repetitive region EB200 and the monoclonal antibody m33G2 have previously been used to characterize the molecule Pf332. These antibodies react with the same high molecular weight polypeptide as were recognized by antibodies raised towards the DBL/nDBL-region of Pf332. The same recognition pattern could be observed in all parasite strains/clones (3D7AH1, 7G8, FCR3S1.2) investigated. The band corresponding to Pf332 is marked with an asterix.
Found at: doi:10.1371/journal.pone.0000477.s003 (0.88 MB TIF)

Figure S4 Schematic model of the role of the DBL-domain of Pf332 during merozoite invasion. A: The DBL-domain of Pf332 is exposed on the late stage iRBC surface and mediates binding to uninfected RBC causing a "late resetting" phenotype. This process provides close proximity of new host cells and facilitates invasion of the released merozoites into new RBC. B: The molecule Pf332 is surface associated. It accumulates during schizont stage and attaches loosely to the merozoites surface assisting the parasite to more easily come in contact with and to invade a new host cell after release from the schizont
Found at: doi:10.1371/journal.pone.0000477.s004 (0.32 MB TIF)

ACKNOWLEDGMENTS

Author Contributions

Conceived and designed the experiments: QC UR KM OK. Performed the experiments: UR AC KM GW MH SN. Analyzed the data: QC UR AC KM OK. Contributed reagents/materials/analysis tools: MW WP KB. Wrote the paper: QC KM.

REFERENCES

1. Gaur D, Mayer DC, Miller LH (2004) Parasite ligand-host receptor interactions during invasion of erythrocytes by *Plasmodium* merozoites. Int J Parasitol 34: 1413–1429.
2. Perkins M (1981) Inhibitory effects of erythrocyte membrane proteins on the in vitro invasion of the human malarial parasite (*Plasmodium falciparum*) into its host cell. J Cell Biol 90: 563–567.
3. Chitnis CE, Blackman MJ (2000) Host cell invasion by malaria parasites. Parasitol Today 16: 411–415.
4. Winter G, Kawai S, Haeggstrom M, Kaneko O, von Euler A, et al. (2005) SURFIN is a polymorphic antigen expressed on *Plasmodium falciparum* merozoites and infected erythrocytes. J Exp Med 201: 1853–1863.
5. Wahlgren M, Carlson J, Udomsangpetch R, Perlmann P (1989) Why do *Plasmodium falciparum*-infected erythrocytes form spontaneous erythrocyte rosettes? Parasitol Today 5: 183–185.
6. O'Donnell RA, Saul A, Cowman AF, Crabb BS (2000) Functional conservation of the malaria vaccine antigen MSP-119across distantly related *Plasmodium* species. Nat Med 6: 91–95.
7. Triglia T, Healer J, Caruana SR, Hodder AN, Anders RF, et al. (2000) Apical membrane antigen 1 plays a central role in erythrocyte invasion by *Plasmodium* species. Mol Microbiol 38: 706–718.
8. Baum J, Maier AG, Good RT, Simpson KM, Cowman AF (2005) Invasion by *P. falciparum* merozoites suggests a hierarchy of molecular interactions. PLoS Pathog 1: e37.
9. Cowman AF, Crabb BS (2006) Invasion of red blood cells by malaria parasites. Cell 124: 755–766.
10. Maier AG, Duraisingh MT, Reeder JC, Patel SS, Kazura JW, et al. (2003) *Plasmodium falciparum* erythrocyte invasion through glycophorin C and selection for Gerbich negativity in human populations. Nat Med 9: 87–92.
11. Gilberger TW, Thompson JK, Triglia T, Good RT, Duraisingh MT, et al. (2003) A novel erythrocyte binding antigen-175 paralogue from *Plasmodium falciparum* defines a new trypsin-resistant receptor on human erythrocytes. J Biol Chem 278: 14480–14486.
12. Glushakova S, Yin D, Li T, Zimmerberg J (2005) Membrane transformation during malaria parasite release from human red blood cells. Curr Biol 15: 1645–1650.
13. Mercereau-Puijalon O, Langsley G, Mattei D (1987) Presence of cross-reacting determinants on several blood stage antigens of *Plasmodium falciparum*. In: "Molecular Strategies of Parasitic Invasion". N Agabian, H Goodman, N Nogueira, eds. UCLA Symposium 42 A R Liss, New York. pp 343–354.
14. Mercereau-Puijalon O, Jacquemot C, Sarthou JL (1991) A study of the genomic diversity of *Plasmodium falciparum* in Senegal. 1. Typing by Southern blot analysis. Acta Trop 49: 281–292.
15. Mattei D, Scherf A (1992) The Pf332 gene of *Plasmodium falciparum* codes for a giant protein that is translocated from the parasite to the membrane of infected erythrocytes. Gene 110: 71–79.
16. Udomsangpetch R, Aikawa M, Berzins K, Wahlgren M, Perlmann P (1989) Cytoadherence of knobless *Plasmodium falciparum*-infected erythrocytes and its inhibition by a human monoclonal antibody. Nature 338: 763–765.
17. Wahlin B, Sjolander A, Ahlborg N, Udomsangpetch R, Scherf A, et al. (1992) Involvement of Pf155/RESA and cross-reactive antigens in *Plasmodium falciparum* merozoite invasion in vitro. Infect & Immun 60: 443–449.
18. Haeggstrom M, Kironde F, Berzins K, Chen Q, Wahlgren M, et al. (2004) Common trafficking pathway for variant antigens destined for the surface of the *Plasmodium falciparum*-infected erythrocyte. Mol Biochem Parasitol 133: 1–14.
19. Mattei D, Berzins K, Wahlgren M, Udomsangpetch R, Perlmann P, et al. (1989) Cross-reactive antigenic determinants present on different *Plasmodium falciparum* blood-stage antigens. Parasite Immunol 11: 15–29.
20. Gardner MJ, Shallom SJ, Carlton JM, Salzberg SL, Nene V, et al. (2002) Sequence of *Plasmodium falciparum* chromosomes 2, 10, 11 and 14. Nature 419: 531–534.
21. Howell DP, Samudrala R, Smith JD (2006) Disguising itself–insights into *Plasmodium falciparum* binding and immune evasion from the DBL crystal structure. Mol Biochem Parasitol 148: 1–9.
22. Marti M, Good RT, Rug M, Knuepfer E, Cowman AF (2004) Targeting malaria virulence and remodeling proteins to the host erythrocyte. Science 306: 1930–1933.
23. Hiller NL, Bhattacharjee S, van Ooij C, Liolios K, Harrison T, et al. (2004) A host-targeting signal in virulence proteins reveals a secretome in malarial infection. Science 306: 1934–1937.
24. Bozdech Z, Llinas M, Pulliam BL, Wong ED, Zhu J, et al. (2003) The transcriptome of the intraerythrocytic developmental cycle of *Plasmodium falciparum*. Plos Biol 1: E5.
25. Llinas M, Bozdech Z, Wong ED, Adai AT, DeRisi JL (2006) Comparative whole genome transcriptome analysis of three *Plasmodium falciparum* strains. Nucleic Acids Res 34: 1166–1173.
26. Pasvol G (2003) How many pathways for invasion of the red blood cell by the malaria parasite? Trends Parasitol 19: 430–432.
27. Mattei D, Scherf A (1992) The Pf332 gene codes for a megadalton protein of *Plasmodium falciparum* asexual blood stages. Mem I Oswaldo Cruz 87 Suppl 3: 163–168.
28. Liang H, Sim BK (1997) Conservation of structure and function of the erythrocyte-binding domain of *Plasmodium falciparum* EBA-175. Mol Biochem Parasitol 84: 241–245.
29. Anders RF (1986) Multiple cross-reactivities amongst antigens of *Plasmodium falciparum* impair the development of protective immunity against malaria. Parasite Immunol 8: 529–539.
30. Udomsangpetch R, Carlsson J, Wahlin B, Holmquist G, Ozaki LS, et al. (1989) Reactivity of the human monoclonal antibody 33G2 with repeated sequences of three distinct *Plasmodium falciparum* antigens. J Immunol 142: 3620–3626.
31. Hinterberg K, Mattei D, Wellems TE, Scherf A (1994) Interchromosomal exchange of a large subtelomeric segment in a *Plasmodium falciparum* cross. EMBO J 13: 4174–4180.
32. Hinterberg K, Scherf A, Gysin J, Toyoshima T, Aikawa M, et al. (1994) *Plasmodium falciparum*: the Pf332 antigen is secreted from the parasite by a brefeldin A-dependent pathway and is translocated to the erythrocyte membrane via the Maurer's clefts. Exp Parasitol 79: 279–291.
33. Ahlborg N, Berzins K, Perlmann P (1991) Definition of the epitope recognized by the *Plasmodium falciparum*-reactive human monoclonal antibody 33G2. Mol Biochem Parasitol 46: 89–95.
34. Ljungström I, Perlmann H, Schlichtherle M, Scherf A, Wahlgren M (2004) Methods in Malaria Research, 4th ed MR4/ATCC Manassas: Virginia, http://www.malaria.atcc.org/MR4_Protocols.html.
35. Flick K, Ahuja S, Chene A, Bejarano MT, Chen Q (2004) Optimized expression of *Plasmodium falciparum* erythrocyte membrane protein 1 domains in Escherichia coli. Malaria J 3: 50.
36. Chen Q, Pettersson F, Vogt AM, Schmidt B, Ahuja S, et al. (2004) Immunization with PfEMP1-DBL1alpha generates antibodies that disrupt rosettes and protect against the sequestration of *Plasmodium falciparum*-infected erythrocytes. Vaccine 22: 2701–2712.
37. Uhlemann R, Staalsoe T, Klinkert M, Hviid L (2000) Analysis of *Plasmodium falciparum*-infected red blood cells. MACS&more 4: 7–8.
38. Pettersson F, Vogt AM, Jonsson C, Mok BW, Shamaei-Tousi A, et al. (2005) Whole-body imaging of sequestration of *Plasmodium falciparum* in the rat. Infect Immun 73: 7736–7746.
39. Pan W, Huang D, Zhang Q, Qu L, Zhang D, et al. (2004) Fusion of two malaria vaccine candidate antigens enhances product yield, immunogenicity, and antibody-mediated inhibition of parasite growth in vitro. J Immunol 172: 6167–6174.

Available online at www.sciencedirect.com
ScienceDirect
Parasitology International 56 (2007) 31–43
www.elsevier.com/locate/parint

The *Plasmodium falciparum* RhopH2 promoter and first 24 amino acids are sufficient to target proteins to the rhoptries

Ahmed Ghoneim [a], Osamu Kaneko [a], Takafumi Tsuboi [b,c], Motomi Torii [a,*]

[a] *Department of Molecular Parasitology, Ehime University Graduate School of Medicine, Shitsukawa, Toon, Ehime 791-0295, Japan*
[b] *Cell-Free Science and Technology Research Center, Ehime University, Matsuyama, Ehime 790-8577, Japan*
[c] *Venture Business Laboratory, Ehime University, Matsuyama, Ehime 790-8577, Japan*

Received 6 October 2006; received in revised form 29 October 2006; accepted 1 November 2006
Available online 15 December 2006

Abstract

The rhoptry secretory organelles of the malaria parasite, *Plasmodium falciparum*, contain a RhopH complex, which is composed of the proteins RhopH1, RhopH2, and RhopH3. RhopH1 is encoded by the *rhoph1/clag* multi-gene family, whereas RhopH2 and RhopH3 are encoded by single-copy genes. The precise function of the RhopH complex has not been identified, but it has been shown that the component proteins are involved in erythrocyte binding and perhaps participate in the formation of the parasitophorous vacuolar membrane. In this study, we have isolated *pfrhoph2* promoter plus the signal peptide encoding sequence and generated transgene expression constructs to evaluate a trafficking and the RhopH complex formation in transgenic *P. falciparum* parasite lines. Interestingly, we found that the N-terminal 24 amino acids of RhopH2, including signal peptide sequence, were sufficient to target GFP to the rhoptries under the *rhoph2* promoter. Because it was previously shown that the timing of the expression alone could not target proteins to the apical organelles, this targeting is likely mediated via a unique mechanism that is dependent on N-terminal 24 amino acids of RhopH2 early in the secretory pathway. The N-terminal one third of Clag3.1, which contains a distinct conserved domain with *Toxoplasma gondii* RON2, can not associate the RhopH complex as a GFP chimera, but a c-Myc-Clag3.1 chimera lacking the C-terminus successfully associates the RhopH complex indicating that cooperation of middle region is likely required but the C-terminus is not necessary.

Keywords: *Plasmodium falciparum*; Rhoptry; RhopH complex; Secretion; Protein targeting

1. Introduction

Plasmodium falciparum is the most potent and deadly species of human malaria parasites, and is responsible for several hundred millions infections and approximately 2 million deaths each year. The morbidity and mortality is exclusively due to blood stream burdens of the intra-erythrocytic stages of the parasite. The erythrocyte-invasive merozoite stages of the parasite use an elaborate apical complex apparatus in order to penetrate the host erythrocyte and establish an enclosing parasitophorous vacuole (PV). In this niche the parasite safely avoids immune surveillance, but acquires nutrients from the erythrocyte cytoplasm and across the erythrocyte surface membrane, for growth, rapid replication, and eventual lysis of the host cell to release merozoites. The merozoite apical secretory apparatus comprises three organelles: the rhoptries, micronemes, and the dense granules, the contents of which play a predominant role in the invasion process and establishment of the PV.

Following the attachment of merozoites to the erythrocyte surface, rhoptry organelles discharge their contents onto the erythrocyte membrane [1]. The rhoptries disappear after erythrocyte invasion and thus are formed *de novo* with each erythrocytic cycle. Rhoptry formation occurs late in the erythrocytic stages of the parasite, at around 40 h after invasion [2]. Elucidation of rhoptry biogenesis of malaria parasites has been hindered by the lack of early organelle markers, and most of our

Abbreviations: aa, amino acid; c-Myc, cellular homologue of myelocytomatosis virus 29 oncogene; *clag*, cytoadherence-linked asexual gene; ER, endoplasmic reticulum; GFP, green fluorescent protein; PBS, phosphate buffered saline; PCR, polymerase chain reaction; PV, parasitophorous vacuole.

* Corresponding author. Tel.: +81 89 960 5285; fax: +81 89 960 5287.
E-mail address: torii@m.ehime-u.ac.jp (M. Torii).

1383-5769/$ - see front matter © 2006 Elsevier Ireland Ltd. All rights reserved.
doi:10.1016/j.parint.2006.11.001

knowledge stems from microscopic examinations of cellular ultrastructure. These studies suggest that rhoptry biogenesis follows the secretory pathway route, and rhoptry organelles are formed by sequential fusion of post-Golgi vesicles [3,4]; although it remains unclear why particular vesicles are selected in the formation of rhoptries [5].

Several merozoite rhoptry components have been identified, including the high molecular mass RhopH complex which consists of three non-covalently associated proteins: RhopH1, RhopH2, and RhopH3 [6–9]. RhopH1 is encoded by three members of the *rhoph1/clag* family, namely, *clag2*, *clag3.1*, and *clag9* [10–12]. The RhopH complex is conserved across *Plasmodium* species and is localized to the rhoptries of mature merozoites, and subsequently retained in the newly formed ring stage parasites following erythrocyte invasion [13]. The function of the complex has not been determined, although it is proposed that the protein complex is involved in erythrocyte binding during or after invasion [14,15], and perhaps participates in the formation of the parasitophorous vacuolar membrane (PVM) [11,13]. It has also recently been proposed that the RhopH complex is a candidate translocon which mediates protein translocation through the PV to the host cell cytoplasm or its surface [16], based upon the finding that in later stages, newly synthesized RhopH2 and RAP3 can also be found in association with Maurer's clefts [17].

Several studies [18–21] have reported that the classical endoplasmic reticulum (ER)-type signal sequence is sufficient for protein recruitment into the secretory pathway within the parasite, and that the PV is the default transit destination for these proteins. These results also imply that targeting to other organelles must require a secondary signal and sorting system. For example, it was recently shown that a Pexel/VTS motif adjacent the signal peptide is required for protein export beyond the PV into the erythrocyte cytoplasm [22,23]. As a second example, apicoplast targeted proteins possess a transit peptide, in addition to the classical ER-signal peptide, for import into the apicoplast [18].

All *Plasmodium* rhoptry proteins analyzed to date contain hydrophobic N-terminal signal peptides, suggesting export via the classical secretory pathway, but thus far no studies have addressed the mechanism of their trafficking and targeting to rhoptries. In this report we exploited the ability to follow the expression of fluorescent proteins in living cells to investigate the signals responsible for the targeting of the RhopH complex proteins to their destination and to explore if the N-terminus of Clag3.1 is responsible for the incorporation of this protein into the complex. Expressing these proteins as chimeras with the green fluorescent protein (GFP) enabled us to visualize rhoptry biogenesis in *P. falciparum*.

2. Materials and methods

2.1. Plasmid constructs

2.1.1. Construction of a basic plasmid vector with a rhoptry gene promoter

The plasmid pHH1 [24] was restriction digested with *Eco*RI and *Hin*dIII to remove the *calmodulin* 5′ untranslated region (UTR), the human *dihydrofolate reductase* (*hdhfr*) ORF, and the *histidine rich protein 3* 3′ UTR. A linker oligonucleotide (AGCTTCCCGGGATCCGTCGACGAATT) that contains the restriction sites *Sma*I, *Bam*HI, and *Sal*I was added to produce the plasmid pH86DT. The *heat shock protein* (*hsp*) *86* 5′ UTR was removed by digesting this plasmid with *Xho*I and *Sma*I and the cohesive end was filled-in using *Taq* DNA polymerase and followed by self-ligation to produce the plasmid pPbDT3U. The regenerated *Xho*I site was then destroyed by *Xho*I digestion and filling in the ends to produce the plasmid pPbDT3UΔX.

To clone a rhoptry gene promoter, *pfrhoph2* 5′ UTR plus the signal peptide encoding sequence was PCR-amplified from 3D7 strain genomic DNA (gDNA) using the forward primer ATACCCCTCGAGTTTTTTGAAAAATATAAAATCGTGC (with *Xho*I site underlined) and the reverse primer ATACCCCTCGAG*ATCCTCTTCTGAGATGAGTTTTTGTT-C*ACTAGTATTCAATTCTAATCCATACAAG which adds *c-myc* epitope sequence (italic) flanked by *Xho*I and *Spe*I sites (underlined). The amplicon included 1027 bp upstream to the start codon and a downstream 69 bp. This amplicon was subcloned into pGEM-T Easy plasmid (Promega, Madison, WI) and the *Xho*I-restriction fragment was ligated into *Sal*I site of pPbDT3UΔX to produce the plasmid pRDT.

pHRPGFPm2 [25] was obtained from K. Haldar through the Malaria Research and Reference Reagent Resource Center, Division of Microbiology and Infectious Diseases, NIAID, NIH and used to amplify GFP with the forward primer ATTGGAAGATCTCTCGAGCCCGGGGCTAGCTC-TAGAAAAGGAGAAGAACTTTTCACTGGAG (with *Bgl*II, *Xho*I, *Sma*I, *Nhe*I, and *Xba*I sites underlined) and the reverse primer ATTGGAAGATCTCTAGTCGACTTTGTA-TAGTTCATCCATGCCA (with *Bgl*II and *Sal*I sites underlined). The amplified DNA fragment was subcloned into pGEM-T Easy, then the *Bgl*II-restriction fragment was ligated into *Bam*HI site of pRDT to produce the plasmid pRGDT (Fig. 1). pRGDT contains *pfrhoph2* 5′ UTR, followed by *pfrhoph2* signal peptide encoding sequence, *Spe*I, *c-myc* tag sequence, multiple cloning site, *gfp* ORF, and *P. berghei* DHFR-TS 3′ UTR (PbDT3′UTR).

The *att*B1 linker (CTAGACAAGTTTGTACAAAAAAG-CAGGCTCTAG) and *att*B2 linker (GGCCACCCAG-CTTTCTTGTACAAAGTGGTGGCC) were inserted into *Avr*II and *Not*I sites, respectively, to convert the plasmid pRGDT into *attB* expression clone (pRGDT-B12), which is ready for the Gateway BP recombination reaction (Invitrogen, Carlsbad, CA) (Fig. 1A).

2.1.2. Construction of the plasmid expressing RhopH2-Myc-Clag3.1$_{(24–483)}$-GFP chimeric protein

To express the N-terminal one third of PfClag3.1 as a chimeric protein fused with c-Myc to its N-terminus and GFP to its C-terminus, we used a pGEM-T Easy clone containing a part of *clag3.1* coding sequence of HB3 strain as a template to amplify the 5′ region encoding the first N-terminal 460 amino acids of the protein after the expected cleavage site of its signal peptide (Fig. 2) using the forward primer

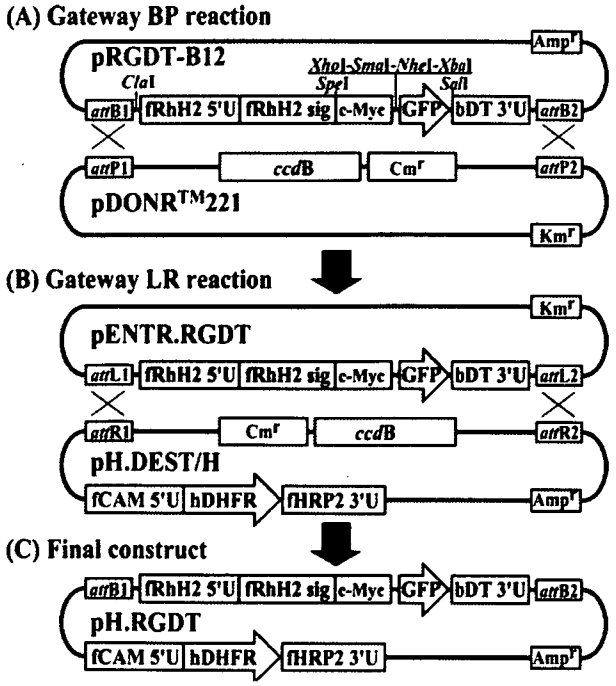

Fig. 1. A schematic diagram of some of the constructs produced in this study. (A) A novel transfection plasmid (pRGDT-B12) with *Plasmodium falciparum pfrhoph2* promoter. Protein of interest would be expressed as a fusion protein with c-Myc tag at its N-terminus and/or GFP at its C-terminus. Several unique restriction sites are available for one-step ligation on both sides of *c-myc* and *gfp* (detail of the one-step ligation is described in the Materials and methods section). The plasmid also contains the Gateway *att*B recombination sites and thus ready to be manipulated by the Invitrogen Gateway technology. This *att*B expression clone was subjected to BP Gateway recombination reaction with the donor vector pDONR™221 to produce the entry clone pENTR.RGDT with *att*L sites (B), which was then subjected to LR recombination reaction with the destination vector pH.DEST/H containing the *att*R sites and the selectable marker *hdhfr* to produce the final transfection construct pH.RGDT (C). pH.RGDT contains the both of the *rhoph2-myc-gfp* expression cassette and the selectable marker *hdhfr* expression cassette.

GTCGACTGTTCAATAAATGAAAATCAAAATGAAAATG (with *Sal*I site underlined) and the reverse primer GTCGACAGATCTTGTATCATAATTTAAAAGTCCAG (with *Sal*I site underlined). The amplicon was subcloned into pGEM-T Easy, and the *Sal*I-restriction fragment was ligated into *Xho*I site of pRGDT-B12 by one-step ligation to produce the plasmid pRGDT-Clag3.1A-B12 (Fig. 1). One-step ligation was performed in a 10 μl reaction mixture (pH 7.9), containing 100 ng of the *Sal*I-restriction fragment, 100 ng of pRGDT-B12, 10 mM Tris–HCl, 10 mM $MgCl_2$, 50 mM NaCl, 1 mM dithiothreitol, 10 ng of BSA, 1 mM ATP, 7 units of *Xho*I, and 200 units of T4 DNA ligase. The reaction mixture was incubated at 16 °C overnight and after inactivation of T4 DNA ligase at 65 °C for 10 min, this mixture was further incubated at 37 °C for several hours for complete digestion of the remaining pRGDT-B12 and transformed into *Escherichia coli* according to the standard protocol. The recombination between *Sal*I-restriction fragment and the *Xho*I-digested plasmid kills *Xho*I site thus rendering the recombined plasmid resistant to digestion whereas the un-recombined plasmid will be easily digested. This enriches the reaction mixture with recombined plasmids.

2.1.3. Construction of the plasmid encoding RhopH2-Myc-Clag3.1Full-GFP chimeric protein

To produce the full length of PfClag3.1 fused with c-Myc to its N-terminus and GFP to its C-terminus, we used pGEM-T Easy clones containing the sequences encoding the middle and C-terminal parts of Clag 3.1 as templates. The middle region of

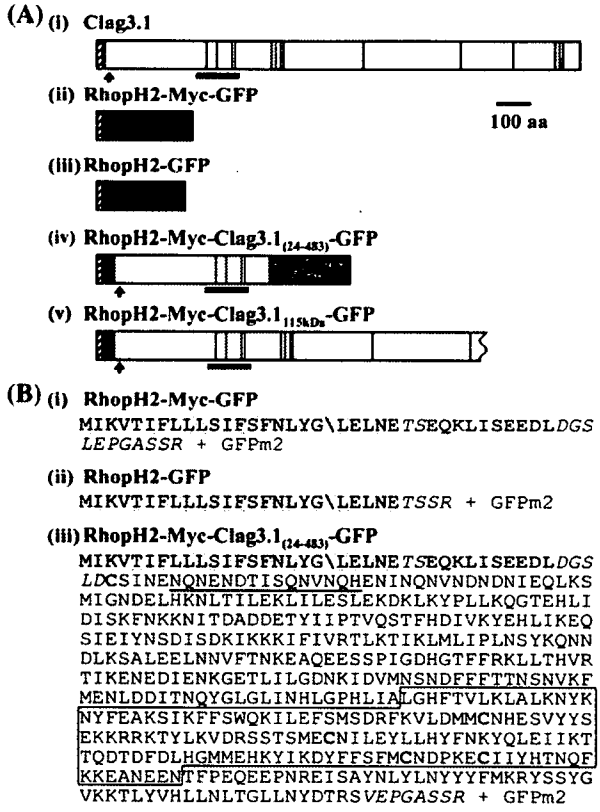

Fig. 2. (A) Structure of the chimeric proteins expressed in transgenic *Plasmodium falciparum*. (i) A schematic diagram of the domain structure of the endogenous Clag3.1. Red vertical lines indicate Cys residues conserved throughout the RhopH1/Clag family and black lines indicate the partially conserved ones. Striped box indicates the putative signal peptide sequence. (ii) RhopH2-Myc-GFP chimeric protein expressed from the transfection construct pH.RGDT. This protein contains the putative signal peptide sequence of PfRhopH2 plus c-Myc and GFP. Blue box represents c-Myc tag and green box represents GFP. (iii) RhopH2-GFP chimeric protein expressed from the construct pH.RGDTΔMyc. (iv) RhopH2-Myc-Clag3.1$_{(24–483)}$-GFP chimeric protein expressed from the construct pH.RGDT-Clag3.1A. This protein contains the putative signal peptide sequence of PfRhopH2 and the amino acids 23–484 of Clag3.1 fused to c-Myc at its N-terminus and GFP at the C-terminus. (v) RhopH2-Myc-Clag3.1$_{115\ kDa}$ which represents a truncated chimeric protein expressed from the construct pH.RGDT-Clag3.1Full. In addition to the putative signal peptide sequence of PfRhopH2 and c-Myc tag at its N-terminus, this protein is estimated to comprise N-terminal 115 kDa of Clag3.1 after the signal peptide cleavage site. Arrows under the schema indicate the target region of rabbit anti-Clag3.1 serum. (B) Amino acid sequence of the GFP chimeric proteins expressed from pH.RGDT (i), pH.RGDTΔMyc (ii), and pH.RGDT-Clag3.1A (iii). Amino acid sequence shaded with gray color represents the putative signal sequence plus 5 amino acids from PfRhopH2 with the back slash indicating the putative cleavage site between Gly_{19} and Leu_{20} as predicted by SignalP 3.0. c-Myc tag sequence is blue in bold, the amino acids introduced for cloning purpose are shown in italic, and the conserved Cys residues are red in bold. Amino acid sequence recognized by rabbit anti-Clag3.1 serum is underlined. Sequence harboring strong homology with PF14_0495 was boxed and indicated in panel Ai with thick bars under the schema. (For interpretation of the references to colour in this figure legend, the reader is referred to the web version of this article.)

clag3.1 was amplified with the forward primer TCGCGGATCC-TATGTGACATCACTTTATTTACCAGG (with *Bam*HI site underlined) and the reverse primer TCGCGGATCCACATAT-CATACATTTTGGATGCTAGC (with *Bam*HI site underlined). The amplicon was subcloned into pGEM-T Easy, sequenced and the *Bam*HI-restriction fragment was ligated by one-step ligation into the endogenous *Bgl*II site that exists in the 3′ end of *clag3.1* gene in the plasmid pRGDT-Clag3.1A-B12 to produce the plasmid pRGDT-Clag3.1AB-B12. The sequence encoding the C-terminal region of Clag3.1 was amplified from the respective pGEM-T Easy clone with the forward primer CTAGTCTAGAATCCAAAATGTATGATATGTTAAATTA-TAA (with *Xba*I site underlined) and the reverse primer CTAGTCTAGAGTGAAATCGTGCGATCATTAATTCATTG (with *Xba*I site underlined). The amplicon was subcloned into pGEM-T Easy, sequenced, and the *Xba*I-restriction fragment was ligated into the endogenous *Nhe*I site that exists in the 3′ end of *clag3.1* gene in the plasmid pRGDT-Clag3.1AB-B12 to produce the plasmid pRGDT-Clag3.1Full-B12.

2.1.4. Preparation of destination vector

pHH1 was digested with *Hpa*I and *Not*I to remove the *hsp86* 5′ UTR and *PbDT* 3′ UTR and after blunting the *Not*I-cohesive end, the Gateway reading frame cassette B containing the *att*R recombination sites (Invitrogen) was ligated to produce the destination vector pH.DEST/H with the *att*R1 recombination site in a head-to-head orientation with human *dhfr* cassette (Fig. 1B).

2.1.5. Gateway recombination reactions

pRGDT-B12, pRGDT-Clag3.1A-B12, and pRGDT-Clag3.1-Full-B12 were subjected to BP recombination reaction with the donor vector pDONR™221 (Invitrogen) according to the manufacturer's instructions to produce the corresponding entry clones pENTR.RGDT, pENTR.RGDT-Clag3.1A, and pENTR.RGDT-Clag3.1Full (Fig. 1A). Then, these entry plasmids were subjected to LR recombination reaction according to the manufacturer's instructions (Invitrogen) with pH.DEST/H to produce the final stable transfection vectors pH.RGDT, pH.RGDT-Clag3.1A, and pH.RGDT-Clag3.1Full (Fig. 1B). Each vector contains 2 expression cassettes in a head-to-head orientation; the gene of interest cassette driven under the control *pfrhoph2* promoter and the human *dhfr* driven under the control of *pfcalmodulin* promoter.

2.1.6. Construction of the plasmid expressing RhopH2-GFP chimeric protein

To express GFP appended to RhopH2 signal peptide and a minimal peptide spacer (Fig. 2), the sequence encoding c-Myc tag and the multiple cloning site were removed by digesting the final transfection vector pH.RGDT directly with *Spe*I and *Nhe*I and self-ligation to produce the vector pH.RGDTΔMyc.

2.2. Parasite culture and transfection

The Dd2 strain of *P. falciparum* was grown *in vitro* essentially under the standard conditions [26]. Parasite transfection was carried out as described previously [27]. Briefly, erythrocytes were washed with incomplete cytomix and loaded with 100 μg of the desired transfection construct using the electroporation system (Bio-Rad, Hercules, CA). Late parasite stages were then inoculated into the plasmid-loaded erythrocytes and parasites were allowed to invade and grow for 3 days before applying the drug WR99210 at 10 nM concentration. Transfected parasites were collected as late schizonts for protein analysis after two rounds of 5% sorbitol treatment. For time course protein analysis, parasites were synchronized using a MACS Type-D depletion column in conjunction with a SuperMACS II magnetic separator (Miltenyi Biotec GmbH, Germany) [28,29]. Culture was passed through the column and schizonts were collected, washed, and inoculated into new uninfected erythrocytes, allowed for rupture and invasion. Four hours later, the culture was passed again through the column and the remaining unruptured schizont-infected erythrocytes were removed and ring stages were allowed to complete a cycle. Equal aliquots of culture were harvested at 0 h and every 8 h thereafter.

2.3. Antibodies

Antibodies used for Western blot analysis and immunoprecipitation were: mouse anti-RhopH2 monoclonal antibody (mAb) 4E10 [13], mouse anti-GFP mAb (GF200; Nacalai, Japan), mouse anti-c-Myc mAb (9E10; Sigma, St. Louis, MO), rabbit anti-Clag3.1 serum, and mouse anti-Clag9 serum [12].

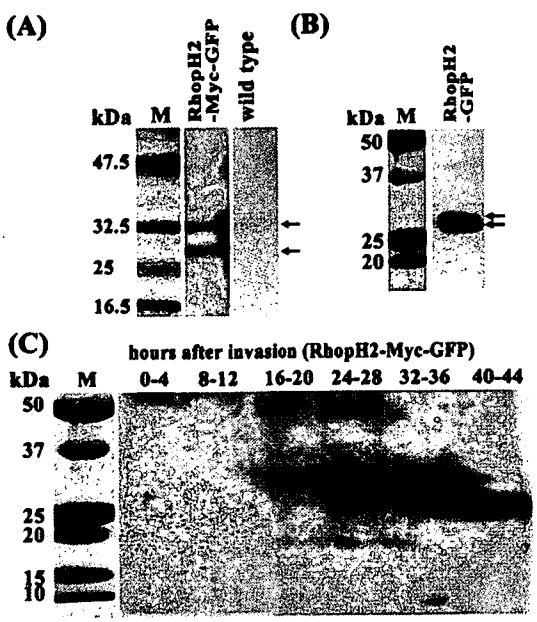

Fig. 3. Western blot analysis of RhopH2-Myc-GFP and RhopH2-GFP chimeric proteins. Proteins were extracted from schizont stage pH.RGDT-transfected parasites and wild type parasites (A) or pH.RGDTΔMyc-transfected parasites (B), and then visualized with anti-GFP mAb on the PVDF membrane after SDS-PAGE. Two bands (32 and 29 kDa; arrows) seen in panel A and 2 overlapping bands (~29 and 27 kDa; arrows) seen in panel B appear to represent the premature and processed forms of the chimeric protein, respectively. (C) Time course of the RhopH2-Myc-GFP chimeric protein expression in the parasites transfected with pH.RGDT over 44 h. Parasites were synchronized to 4 h window, and then harvested every 8 h after erythrocyte invasion for 1 complete cycle.

Antibodies used for immunofluorescence assay were: rabbit anti-Clag9 serum [11], rabbit anti-AMA1 serum (a kind gift from C. Long) and anti-GFP mAb (JL-8; BD living colors).

2.4. Western blot analysis

Parasite proteins were extracted by repeated freeze–thaw cycles, dissolved in 1× SDS-PAGE loading buffer and run on 5–20% polyacrylamide gel (ATTO, Japan) after incubation at 100 °C for 3 min. Proteins were blotted onto a 0.22 μm PVDF membrane (Bio-Rad) and immunostained with the specific primary antibodies or antisera followed by horseradish peroxidase-conjugated secondary antibody staining (Biosource Int., Camarillo, CA) and visualized with ECL Plus (Amersham Biosciences, UK) on RX-U film (Fuji, Japan).

2.5. Immunoprecipitation analysis

Immunoprecipitation was carried out as described previously [30]. Briefly, proteins were extracted from late schizont parasite pellets by repeated freeze–thaw cycles in PBS containing a cocktail of proteinase inhibitors. Supernatants (100 μl) were pre-incubated for 1 h at 4 °C with 40 μl of 50% protein G-conjugated beads (GammaBind Plus Sepharose; Amersham Biosciences) in NETT buffer (50 mM Tris–HCl, 0.15 M NaCl, 1 mM EDTA, and 0.5% Triton X-100) supplemented with 0.5% BSA (fraction V; Sigma). Recovered supernatants were incubated with rabbit anti-PfRhopH2 serum [7] or mouse anti-c-Myc mAb (9E10) with gentle rotation for 2 h at 4 °C and then 40 μl of 50% protein G-conjugated beads were added. After 1 h incubation at 4 °C, the beads were washed once with NETT-0.5% BSA, once with NETT, once with high-salt NETT (0.5 M NaCl), once with NETT, and once with low-salt NETT (0.05 M NaCl and 0.17% Triton X-100). Finally, proteins were extracted from the protein G-conjugated beads by incubation with SDS-PAGE loading buffer at 100 °C for 3 min. Supernatants were collected and stored at −70 °C until next day for Western blot analysis.

2.6. Immunofluorescence assay and microscopy

For GFP imaging, small aliquots of parasite culture were washed with PBS, incubated in PBS containing 4′, 6-diamidino-2-phenylindole (DAPI) for 5 min and then mounted without further treatment. Parasites expressing GFP were imaged using a fluorescence microscope (BX50; Olympus, Japan) and digital camera (IM500; Leica, Germany). Immunofluorescence assay was performed in the same way as described previously [12]. Briefly, schizont-rich infected erythrocytes were smeared on glass slides and stored at −80 °C until use. Later, smears were fixed in ice-cold acetone, pre-incubated with PBS containing 5% non-fat milk at 37 °C for 30 min and reacted with the desired primary antibody at 37 °C for 1 h. Smears were then washed with PBS and reacted with fluorescein isothiocyanate (FITC)-conjugated goat anti-(mouse IgG and IgM) secondary antibody (Biosource Int.) and Alexa546-conjugated

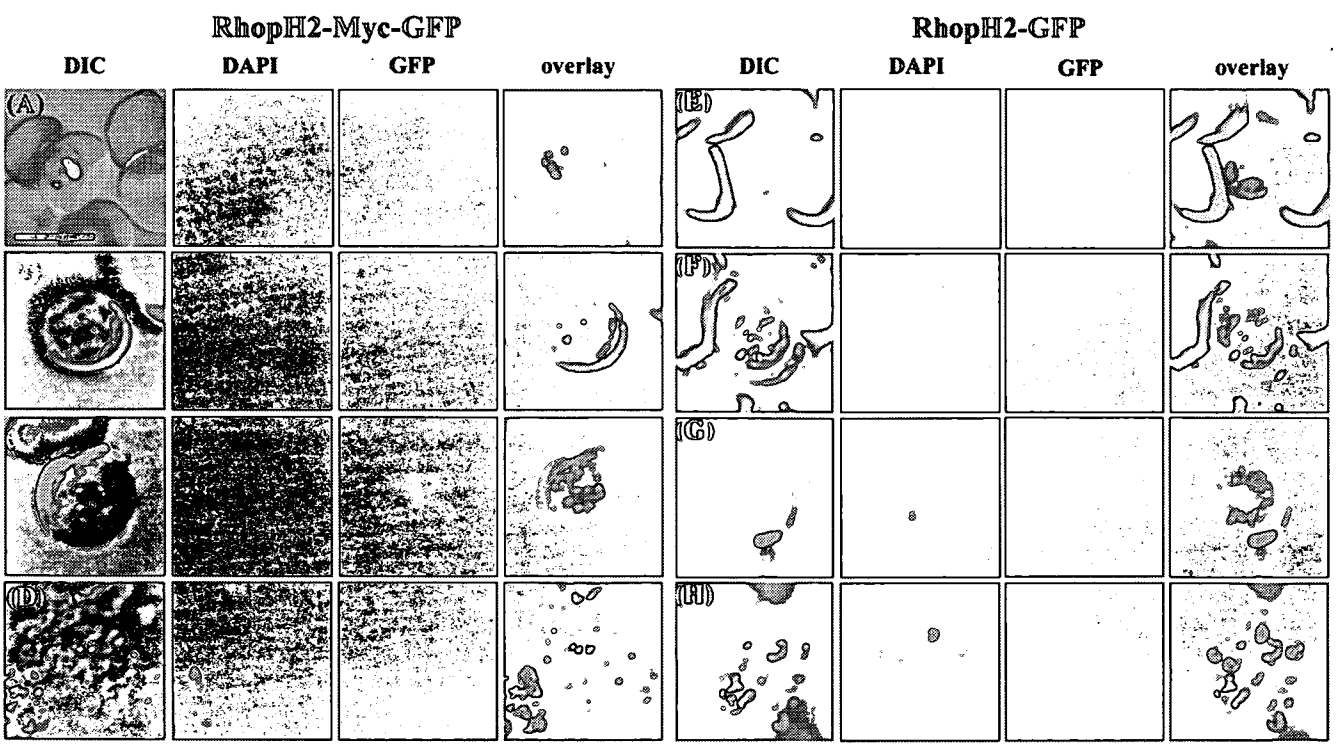

Fig. 4. Similar trafficking and subcellular localization of RhopH2-Myc-GFP (A–D) and RhopH2-GFP (E–H) chimeric proteins during late developmental stages of parasite growth. Images were collected from live parasites. (A and E) Early schizont stages showing almost even fluorescence signal in the cytoplasm and probably the parasitophorous vacuole. (B and F) Further developed schizonts showing accumulation of the chimeric proteins around the parasites. (C and G) Later schizont stages showing fluorescence surrounding individual merozoites. Fluorescent vesicles can be seen; probably representing premature rhoptries. (D and H) Segmented schizonts showing concentrated fluorescence signal at the apical end of the formed merozoites. Nuclei were stained with DAPI. Scale bar represents 5 μm.

goat anti-rabbit-IgG (H+L) secondary antibody (highly cross-adsorbed; Molecular Probes, Eugene, OR) at 37 °C for 30 min. Images were captured as described above. Nuclear staining was performed using DAPI, the slides were mounted in ProLong antifade reagent (Molecular Probes), and images were processed using Adobe Photoshop software.

3. Results

3.1. Construction of a novel transfection vector with a rhoptry gene promoter

To study the protein trafficking of rhoptry proteins we constructed a vector, pRGDT-B12, which expresses proteins of interest fused to the RhopH2 signal peptide sequence and under the control of the rhoptry gene *pfrhoph2* promoter. The signal peptide sequence of the expressed fusion proteins is predicted to be cleaved between Gly_{19} and Leu_{20} (Fig. 2). As a mean to determine the cellular localization, the expressed proteins contain a c-Myc epitope downstream of the signal peptide and GFP at their C-terminus. The c-Myc epitope and GFP are both flanked by unique restriction sites for manipulation such that either can be removed from the expressed fusion proteins. The multiple unique restriction sites (*Xho*I, *Sma*I, *Nhe*I, and *Xba*I) between the c-Myc tag and GFP allow for a convenient one-step ligation reaction that does not require pre-digestion of the plasmid backbone. Variable restriction-fragments can be ligated into one restriction site (e.g. *Avr*II, *Spe*I, or *Xba*I-restriction fragments can be ligated into *Nhe*I site) with similar procedure to the ligation of *Sal*I-restriction fragment into *Xho*I site as used to generate pRGDT-Clag3.1A-B12 (see Material and methods). All components described above in pRGDT-B12 were flanked by the *att*B1 and *att*B2 Gateway recombination sites making it ready to recombine with the desired destination vector possessing a suitable selectable marker according to the Gateway technology. pRGDT-B12 with the carefully designed multiple cloning site provides more flexibility than the entry vector (pENTR.RGDT).

3.2. Characterization of the pfrhoph2 promoter

To confirm the ability of the *pfrhoph2* promoter to drive episomal expression of inserted gene sequences, we transfected *P. falciparum* with the plasmid pH.RGDT and generated a parasite line retaining the plasmid as a stable episome. Western blot analysis of late schizont stage transformants using anti-GFP serum showed two clear bands at 32 kDa and 29 kDa (Fig. 3A) that are specific to transfected parasites. The 32-kDa band corresponds to the expected size of the unprocessed RhopH2-Myc-GFP chimeric protein expressed from pH.RGDT, whereas the 29-kDa band is consistent with the size expected for the mature protein after cleavage of the signal peptide sequence (Fig. 2A).

To evaluate the timing of protein expression under the *pfrhoph2* promoter, the transfected parasites were synchronized using a MACS apparatus and the 4 h-window parasites were collected every 8 h for Western blot analysis (Fig. 3C). Proteins collected at the ring stages (0–4 and 8–12 h) did not show any signal with anti-GFP serum. A single faint 32-kDa band corresponding to the size of the unprocessed protein form was detected from early trophozoite stage (16–20 h). The amount of the unprocessed chimeric protein gradually increased until it reached a peak at schizont stage (32–36 h), then it ceased dramatically in the mature schizont stage (40–44 h). Another

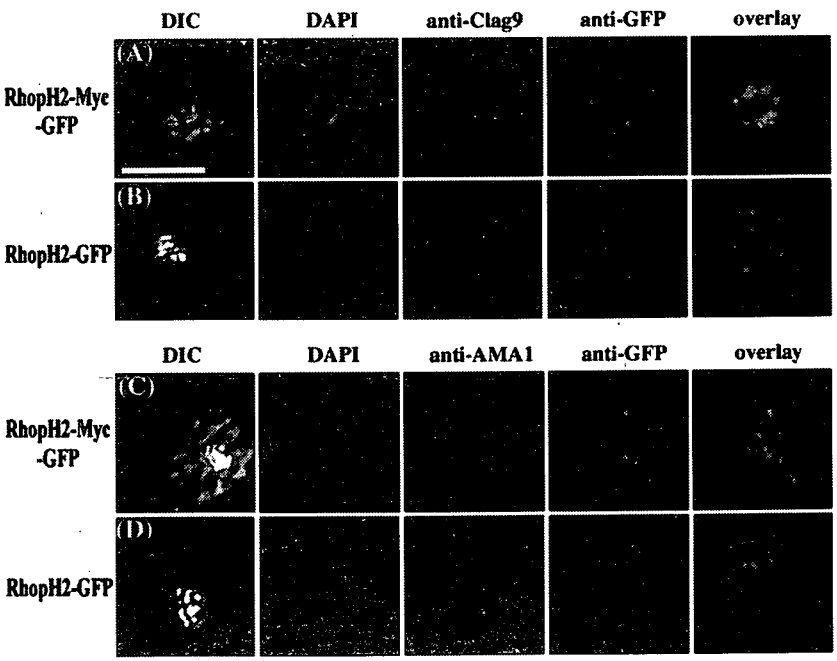

Fig. 5. Co-localization of GFP chimeric proteins with the rhoptry protein Clag9 but not with the microneme protein AMA1. (A and C) Late schizonts expressing RhopH2-Myc-GFP chimeric protein. (B and D) Late schizonts expressing RhopH2-GFP chimeric protein. Air-dried segmented schizonts were fixed with acetone and reacted with anti-GFP mAb, and rabbit anti-Clag9 serum or rabbit anti-AMA1 serum. Nuclei were stained with DAPI. Scale bar represents 5 μm.

faint but discrete 29-kDa band corresponding to the size of the mature protein form was detected in late trophozoite stage (24–28 h). The amount of the mature form gradually increased until the end of the asexual life cycle (40–44 h) when its peak expression was observed. The expression pattern shown here may suggest a post-translational recruitment of the fusion protein into the ER. Although expression of the chimeric protein here seems to be slightly earlier when compared to the transcription of native *rhoph2*, which was detected after 30 h post-invasion [11], our results show that RhopH2-Myc-GFP chimera was correctly processed and showed peak expression at the mature schizont stage. This validates the use of *pfrhoph2* promoter in studying the proteins that are expressed in late schizont stage.

3.3. The RhopH2 promoter and first 24 amino acids are sufficient to target proteins to the rhoptries

Transgenic *P. faciparum* parasite line that express RhopH2-Myc-GFP chimeric protein showed strong green fluorescence during the schizont stage of the parasite growth. The expressed chimeric protein consists of the ER signal peptide sequence plus a short linker sequence and c-Myc tag and GFP (Fig. 2Bi). No fluorescence signal was detected in ring or trophozoite stages, whereas early schizont stage parasites showed uniform green fluorescence throughout the cell and maximal expression at the periphery of the parasite (Fig. 4A). This fluorescence pattern is consistent with chimeric protein localization within the parasite cytoplasm and likely the PV. As the intra-erythrocytic parasites matured (Fig. 4B), the fluorescence signal increased in specific marginal areas. In mature parasites a segmented fluorescence pattern surrounding the individual merozoites was observed, which again is consistent with trafficking of the proteins to the PV (Fig. 4C). Some vesicles can be seen within individual immature merozoites, which might be immature rhoptry vesicles. In the segmented schizonts, the fluorescence signal was clearly localized at the apical end and the fluorescence surrounding the merozoites disappeared, probably because the erythrocyte and PV membranes were partly ruptured (Fig. 4D). This pattern was repeatedly observed with no obvious differences despite an extensive investigation of a large number of schizonts.

Foth et al. [31] has shown that targeting proteins to the apicoplast is influenced by the acidic amino acids downstream to the signal peptide. To evaluate whether this is the case, we generated *P. falciparum* parasite line expressing a chimeric protein RhopH2-GFP by transfecting with pH.RGDTΔMyc. This chimeric protein lacks c-Myc tag and contains only 9 amino acids (LELNETSSR) between the RhopH2 signal peptide and GFP (Fig. 2Bii). Thus, this chimeric protein lacks 6 out of the 8 acidic amino acids existing in RhopH2-Myc-GFP chimera and, in total, 7 charged amino acids out of 10 were removed. Western blot analysis of the RhopH2-GFP chimeric protein revealed 2 overlapping bands (~29 and 27 kDa) that appear to represent the premature and processed forms of the chimeric protein, respectively (Fig. 3B). Trafficking pattern of RhopH2-GFP during the erythrocytic cycle was identical to that of RhopH2-Myc-GFP (Fig. 5E–H). These data indicate that both GFP chimeric proteins were similarly expressed in the cytoplasm at early schizont stage; and later, during merozoite formation, these proteins were translocated to the apical end of the newly formed merozoites in the late schizont stage parasite, suggesting that these proteins are targeted to a specific apical organelle.

To evaluate the subcellular localization of GFP-chimeric proteins in late schizont stages, we performed a double immunofluorescence staining assay on mature segmented schizont stage parasites using an anti-GFP mAb plus rabbit anti-Clag9 serum or rabbit anti-AMA1 serum. For both parasite lines, the GFP-chimeric proteins were co-localized with Clag9, an authentic rhoptry protein, but were not co-localized with AMA1, an authentic microneme protein. This suggests that both GFP-chimeric proteins were successfully targeted to the rhoptries, but not to the micronemes. Thus, the first 24 amino acids of RhopH2 including signal peptide sequence is sufficient to target proteins to the rhoptries under the *rhoph2* promoter sequence.

3.4. Expression of RhopH2-Myc-Clag3.1$_{(24-483)}$-GFP chimeric protein

The RhopH1/Clag protein family members possess an N-terminal domain that contains 4 conserved Cys residues. A TBLASTN search of the *P. falciparum* genome sequence

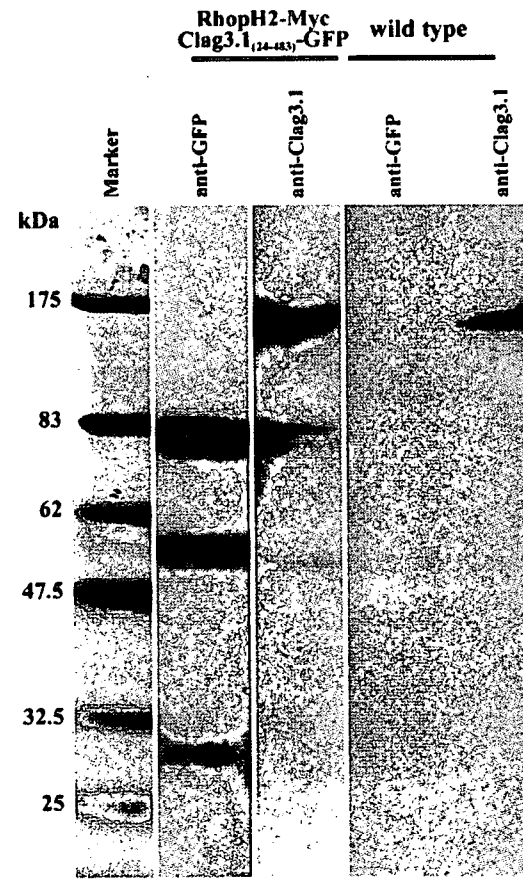

Fig. 6. Western blot analysis of the RhopH2-Myc-Clag3.1$_{(24-483)}$-GFP chimeric protein. Proteins were extracted from schizont stage pH.RGDT-Glag3.1A-transfected parasites and wild type parasites, and then visualized with anti-GFP mAb or anti-Clag3.1 serum on the PVDF membrane after SDS-PAGE.

database, using the Clag2 amino acid sequence as a query, identifies this domain within an additional ORF (PF14_0495 in PlasmoDB) that is most similar to the N-terminus of Clag2 (Fig.2) and represents a discrete domain of unknown function. Based on this domain prediction and because the Clag3.1 domain responsible for associating the other components of the RhopH complex is unknown, we selected the N-terminal one third of Clag3.1 (Fig. 2) to evaluate if this region is responsible for its involvement in the high molecular weight RhopH complex. To this end, we generated the transfection vector pH. RGDT-Clag3.1A that would express Clag3.1 (aa 24–483) as a chimeric protein with PfRhopH2 signal peptide and c-Myc tag at its N-terminus and GFP at its C-terminus (RhopH2-Myc-Clag3.1$_{(24–483)}$-GFP; Fig. 2Aiv). This construct was used to generate a parasite line retaining the plasmid as a stable episome.

The integrity of the expressed chimeric protein was confirmed by Western blot analysis of transfected parasite extracts using mouse anti-GFP mAb and rabbit anti-Clag3.1 serum that recognizes aa 29–43 of Clag3.1. As shown in Fig. 6, anti-GFP mAb recognizes three bands with sizes of approximately 82, 54, and 28 kDa. In contrast, the anti-Clag3.1 serum identified three bands having molecular weights of roughly 153,

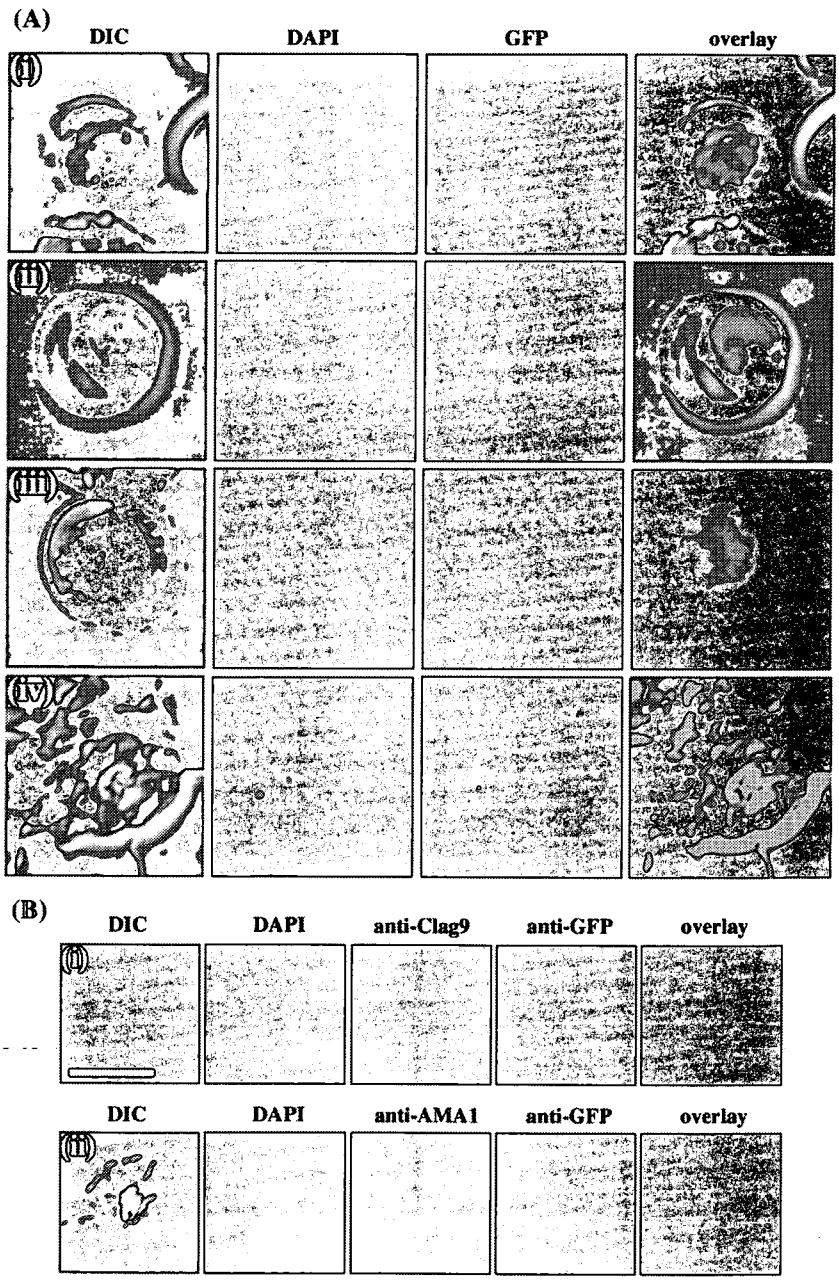

Fig. 7. Characterization of the parasites expressing the RhopH2-Myc-Clag3.1$_{(24–483)}$-GFP chimeric protein. (A) Trafficking and subcellular localization of RhopH2-Myc-Clag3.1$_{(24–483)}$-GFP chimeric protein during the late stages of parasite growth is identical to those of RhopH2-Myc-GFP and RhopH2-GFP chimeric proteins shown in Fig. 4. Images from early schizont stage (i), further developed schizont (ii), later schizont stage (iii), and segmented schizont (iv) are shown. Nuclei were stained with DAPI. (B) The RhopH2-Myc-Clag3.1$_{(24–483)}$-GFP chimeric protein co-localized with the rhoptry protein Clag9 (i), but not with the microneme protein AMA1 (ii). Scale bar represents 5 μm.

82, and 80 kDa. The band in common with the two antisera, of 80–82 kDa molecular weight, is consistent with the expected size of the unprocessed and mature forms of the chimeric protein (Fig. 2Biii). Thus, the chimeric protein possessing Clag3.1 N-terminus appears to be correctly targeted to the ER, and the signal peptide is cleaved. The 54-kDa band detected with anti-GFP mAb is likely a truncated form of the chimeric protein and the 28-kDa band corresponds to the size of a GFP that might have been cleaved from the chimeric protein. The 153-kDa band detected with anti-Clag3.1 serum corresponds to the size of the endogenous Clag3.1. The rabbit anti-Clag3.1 serum identifies a single 153-kDa band in the wild type parasite extracts, which is consistent with the size of the endogenous Clag3.1; whereas the anti-GFP mAb does not recognize proteins in the wild type parasite extracts.

Following the expression of this chimeric protein during the erythrocytic cycle showed identical trafficking pattern to those of RhopH2-Myc-GFP and RhopH2-GFP, which ended with the translocation of this chimera to the apical end of the newly formed merozoites in the late schizont stage parasites (Fig. 7A, rows i–iv). The double immunofluorescence assay performed in the same way as above confirmed that this chimeric protein was specifically targeted to the rhoptries (Fig. 7B).

3.5. The N-terminal one third of Clag3.1 can not associate with the RhopH complex as a GFP chimeric protein

To determine if the conserved domain located in the N-terminal region of Clag3.1 contributes to the RhopH complex formation, we performed immunoprecipitation assays using protein extracts from transgenic parasites expressing the RhopH2-Myc-Clag3.1$_{(24-483)}$-GFP chimeric protein. The PfRhopH complex was immunoprecipitated with rabbit anti-RhopH2 serum and Western blot was performed with anti-RhopH2 mAb 4E10, mouse anti-Clag9 serum, and anti-GFP mAb. The chimeric protein was not detected following immunoprecipitation, whereas RhopH2 and Clag9 were successfully detected in the immunoprecipitated RhopH complex (Fig. 8). This indicates that the chimeric protein possessing the N-terminal 460 amino acids of Clag3.1 is incapable of associating with the RhopH complex as GFP-chimeric protein.

3.6. The C-terminus of Clag3.1 is not necessary for associating the RhopH complex

Aiming to generate positive control to investigate the Clag3.1 region possessing a RhopH complex-associating motif, we generated the transfection vector pH.RGDT-Clag3.1-Full which encodes the full length of Clag3.1 as a fusion protein with c-Myc at its N-terminus and GFP at its C-terminus. Transgenic parasites maintaining this construct as a stable episome did not show any green fluorescent signal when examined alive. Western blot analysis of transfected parasite extracts using mouse anti-GFP mAb did not show any signal. However, probing the same parasite extract with mouse anti-c-Myc mAb recognized one clear 120-kDa band (Fig. 9A). Probing non-transfected parasite extracts with anti-c-Myc did

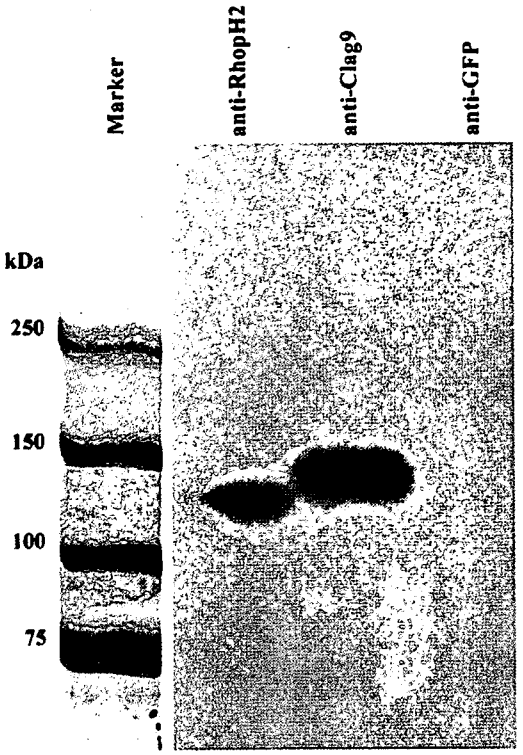

Fig. 8. Western blot analysis of the PfRhopH complex immunoprecipitated with rabbit anti-RhopH2 serum. Membranes were probed with mouse anti-RhopH2 (mAb 4E10), mouse anti-Clag9, or anti-GFP mAb. Both of RhopH2 and Clag9 were successfully detected, while the RhopH2-Myc-Clag3.1$_{(24-483)}$-GFP chimeric protein was not.

not show any signal (not shown). Thus, the 120-kDa band represents a truncated Clag3.1 that retains c-Myc at its N-terminus but lost GFP plus a 40-kDa C-terminal region of Clag3.1 (Fig. 2). Hence this chimeric protein was designated RhopH2-Myc-Clag3.1$_{115\ kDa}$. Nucleotide substitutions were evaluated by sequencing plasmids recovered from the transfected parasite line, however, no substitution resulting frame-shift and/or stop codon were found. Thus, the inability to detect GFP plus the 40-kDa C-terminal region suggests that this small Clag3.1-GFP chimera has been degraded immediately after expression. Another possibility could be a translational arrest during the expression of this long chimeric protein, in this case around 184 kDa, from an episomal plasmid.

To investigate whether the RhopH2-c-Myc-Clag3.1$_{115\ kDa}$ can associate the RhopH complex, we immunoprecipitated RhopH complex with rabbit anti-RhopH2 serum and probed with anti-c-Myc mAb. The chimeric protein was successfully detected in the immunoprecipitated complex in addition to RhopH2 and Clag9, the positive controls (Fig. 9B). Reciprocally, we immunoprecipitated RhopH complex with anti-c-Myc mAb and probed with rabbit anti-RhopH2 serum, rabbit anti-Clag9 serum, anti-c-Myc mAb, and rabbit anti-Clag3.1 serum. RhopH2 was successfully co-precipitated with the chimeric protein, but Clag9 and the endogenous Clag3.1 were not co-precipitated. These data indicate that the C-terminus of Clag3.1 is not necessary for associating the RhopH complex. In

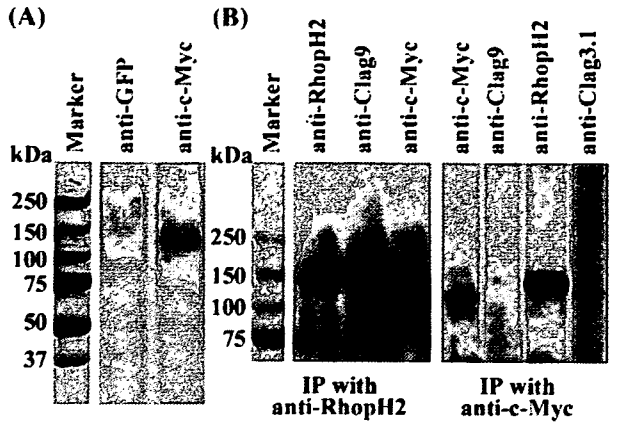

Fig. 9. Western blot analysis of the RhopH2-Myc-Clag3.$1_{115\ kDa}$ chimeric protein and the immunoprecipitated PfRhopH complex. (A) A single 120-kDa band was detected in the extracts from schizont stage parasites transfected with the construct pH.RGDT-Glag3.1Full with anti-c-Myc mAb, but not with anti-GFP mAb. (B) PfRhopH complex was immunoprecipitated with rabbit anti-RhopH2 serum and probed with mouse anti-RhopH2 (mAb 4E10), mouse anti-Clag9, or anti-c-Myc mAb. RhopH2-Myc-Clag3.$1_{115\ kDa}$ was successfully co-precipitated with RhopH2. In case of reciprocal immunoprecipitation of the PfRhopH complex with anti-c-Myc mAb, membranes were probed with rabbit anti-RhopH2 serum, rabbit anti-Clag9, anti-c-Myc mAb, or rabbit anti Clag3.1. In this case too, RhopH2 was successfully co-precipitated with RhopH2-Myc-Clag3.$1_{115\ kDa}$ but neither Clag9 nor the endogenous Clag3.1 was detected in this complex.

addition, the incorporation of RhopH2-c-Myc-Clag3.$1_{115\ kDa}$ into the RhopH complex prevented the incorporation of Clag9 and Clag3.1 into the same RhopH complex, supporting the previous proposal that each RhopH complex contains only one RhopH1/Clag family member [12].

4. Discussion

To study rhoptry protein expression and trafficking we have developed new transfection vectors for manipulating *Plasmodium* rhoptry proteins as GFP chimeras. Our results show that targeting proteins to the rhoptries follow the secretory pathway and only N-terminal 24 amino acids including a signal peptide sequence and correct expression timing are sufficient. Before being targeted to the rhoptries, proteins expressed from our constructs were seen accumulated in a cellular compartment that is likely the PV. We also showed that the C-terminus of Clag3.1 is not necessary for associating the RhopH complex.

The vector pRGDT-B12 developed in this study was designed to allow the production of tagged proteins with either or both c-Myc and GFP. The vector can be manipulated by the Gateway technology and allows easy cloning of genes of interest by single step ligation reactions that are faster and more efficient than the conventional ligation procedures. The resultant chimeric protein is expressed under the control of the *pfrhoph2* promoter. Due to the high AT content in *P. falciparum* genome, especially in the intergenic regions (86.4% AT content), the promoter sequences cloned from this pathogen are still very few and so far there is no report about cloning of any rhoptry gene promoter. Expression of the transgene under the *rhoph2* promoter was shown to be maximal in schizont stages. The precise timing of transgene expression has been shown to be critical for correct trafficking and subcellular localization of transgene products [32,33]; and thus these expression vectors will serve as valuable tools in studying the trafficking and expression of rhoptry and other proteins that are expressed in the late intra-erythrocytic parasite stages. The slightly earlier expression of the transgene could be due to a leaky expression from the *rhoph2* promoter in the episomal context, or due to the lack of additional upstream promoter elements needed for very tightly controlled timing of expression [32]. Notably, GFP fluorescence was detected only in schizont stages, and thus high levels of translated protein are relegated to mature intra-erythrocytic stages.

To explore the mechanism of protein targeting to rhoptries, we produced two GFP-expressing stable parasite lines and followed the trafficking pattern of GFP. Since, all proteins identified or predicted to be secreted from the apical organelles, rhoptries and micronemes, contain N-terminally located ER signal peptide sequence, we first showed by Western blot analysis that GFP fused to c-Myc and the signal peptide of RhopH2 appeared to be retained as an immature form, then later ER signal peptide was cleaved. This indicates that GFP fused with RhopH2 signal peptide is translocated to the ER post-translationally and this feature may reflect a specific nature of the RhopH2 signal sequence. According to Schatz and Dobberstein [34], the signal sequence mediates not only recognition of a protein by the membrane-linked transport system, but it can also have other functions such as determining whether transport into the ER occurs co- or post-translationally [35].

Our data conclusively show that RhopH2 signal peptide sequence plus only 5 amino acids downstream to the signal peptide cleavage site are able to target GFP to the rhoptries under the *rhoph2* promoter. Recently, Treeck et al. [36] showed that GFP fused with N-terminal 36 amino acids of microneme protein EBA-175 including predicted signal peptide sequence (21 aa), followed by EBA-175 transmembrane domain were not able to target to the apical organelle under *ama1* promoter, for which maximal expression can be seen at schizont stage, similar timing to the *rhoph2* promoter. This observation suggests that the timing of the expression is not the definitive factor of the rhoptry targeting. There are no reports of rhoptry targeting signal in *Plasmodium*, but at least 2 cases have been reported in the other apicomplexan parasite, *Toxoplasma gondii*. For example, TgROP1 can be targeted to the rhoptries with either the propeptide region (aa 1–85) including ER signal peptide sequence or a 372 amino acid central fragment [37]. Another case is TgROP4, for which the rhoptry targeting was originally proposed to be mediated by a C-terminal Tyr-based motif (YXXø) [38], but recent report showed that the N-terminal 163 amino acids, including ER signal peptide sequence, is sufficient for directing a GFP fusion protein to the rhoptries [39]. Together with these reports, our results suggest that N-terminal sequence around signal peptide have the capacity to target rhoptry proteins to their destination when expressed at schizont stage.

In *E. coli*, the signal sequence can act as a true targeting signal because it is specifically recognized by a cytosolic chaperone or targeting factor [34]. For example, the translocation of periplasmic alkaline phosphatase and maltose binding protein was suggested to depend on the chaperone DnaK

(*E. coli* homologue of Hsp70) [40] and the hydrophobic signal sequences of these proteins were found to constitute DnaK binding sites suggesting that the role of DnaK in translocation of these proteins relies on direct association with the signal sequence [41]. In yeast, a member of the Hsp70 family in the ER termed BiP is bound to a lumenally exposed DnaJ-like domain of Sec63p, a transmembrane subunit of the Sec63 complex [42–44]. This Hsp70 on the inner side of the ER membrane interacts with the translocating polypeptide chain and pulls it across the membrane [For details, see Refs. [34,45]]. In *P. falciparum*, mutating some amino acid residues predicted to be a part of the chaperone binding sites preceding the conserved host cell targeting motif (HCT or PEXEL motif) resulted in a significant retention of a portion of the chimeric STEVOR protein within the parasite's ER [46]. Similarly, the putative Hsp70 (DnaK) binding sites present in the transit peptide proved to be important for correct targeting of proteins to the apicoplast [31]. These results imply an auxiliary or alternative role for parasite chaperones in protein targeting. The study of Sargeant et al. [47] to predict the exported proteins in the genus *Plasmodium*, showed the presence of chaperone binding sites in many of the well known and predicted exported proteins families together with a family of putative DnaJ domain-containing co-chaperones, implying a role for these co-chaperones in the translocation process and correct conformation of some of these proteins (e.g. PfEMP1 complex).

Based on the above-mentioned reports, we suggest that the chimeric proteins in this study were recognized by a chaperone, for example Hsp70 family or its homologues, in the ER matrix through interaction with the first 24 amino acid sequence of the RhopH2 including signal peptide. A simultaneous binding to the mature proteins by a specific co-chaperone or co-factor would then mark these proteins for binding with a rhoptry-targeted molecule. In fact, Topolska et al. [5] has identified a rhoptry protein RAMA (rhoptry-associated membrane antigen) that is synthesized several hours before rhoptry formation (the earliest expressed rhoptry protein) and transiently localizes within the ER and Golgi within lipid-rich microdomains and some other rhoptry proteins such as RhopH3 and RAP1 were found in close apposition with RAMA.

The accumulation of both of the chimeric proteins in the PV of the schizont stages before the appearance of any rhoptry vesicles shows a typical "necklace-of-beads" pattern described for the PV localization of GFP chimeras of the exported proteins KAHRP, Exp1, and RESA [19,21,32]. Such pattern was suggested to represent either vesicular compartments involved in the transport of the fluorescent protein to the PV, or subcompartments within the PV [19]. Recent reports suggested that rhoptry proteins might have a function in the PV before rhoptry formation. For example, RhopH3 was transiently localized to the PV before rhoptry formation [48] and the proteome analysis identified newly synthesized rhoptry proteins, RhopH2 and RAP3, in the membranous network fraction [17]. Based on these data, the RhopH complex was proposed to be a possible candidate translocon mediating export of proteins through the PV [16]. Whether these accumulations are just default depot as reported [18,19,21,32] due to an earlier timing of expression of our chimeric proteins before rhoptry formation or for a functional role in the PV is yet to be determined.

In this report, we evaluated, for the first time, the role of a recognizable conserved domain in the RhopH complex formation. This domain is located at the N-terminus of RhopH1 and has apparent homology with PF14_0495. PF14_0495 is encoded in single exon and an orthologous protein TgRON2 was recently identified in *T. gondii* and proposed to make a complex including TgAMA1 [49,50]. The results presented here show that RhopH2-Myc-Clag3.1$_{(24-483)}$-GFP chimeric protein can not associate the RhopH complex and the C-terminus of Clag3.1 is not necessary for associating the RhopH complex. We should note that there is a possibility that a potential RhopH complex association of the Clag3.1$_{(24-483)}$ part might be interfered by fusing with GFP. The C-terminal part of the chimeric Clag3.1 is estimated to be chopped off after the eleventh Cys residue in Clag3.1 which represents the tenth and the last Cys residue conserved among all members of RhopH1/Clag family. With respect to amino acid sequence conservation among parasite lines, members of the RhopH1/Clag family show most of the variation in the C-terminus [unpublished data]. Thus, the region where the RhopH complex-associating motif locates appears to be conserved among parasite lines.

In summary, we have expressed GFP and Clag3.1-GFP as fusion proteins with RhopH2 signal peptide under *rhoph2* promoter to show that targeting of the rhoptry proteins is mediated by unknown mechanism probably involving the interaction of some chaperones with RhopH2 signal peptide early in the ER and the interaction of rhoptry-targeted molecules. Incorporation into the RhopH complex can not be accomplished by the interaction of the N-terminal one third of Clag3.1 as a GFP chimera but a truncated Clag3.1 lacking the C-terminal region successfully associated the RhopH complex suggesting that cooperation of the middle region is probably required and that the C-terminus of Clag3.1 is not necessary for the RhopH complex formation.

Acknowledgements

We thank T. Templeton for the critical reading and helpful comments. We are grateful to A. Cowman for providing pHH1, D. Jacobus for WR99210, A. Holder and I. Ling for rabbit anti-PfRhopH2 serum and mAb 4E10, C. Long for rabbit anti-AMA1 serum and D. Mattei for rabbit anti-Clag9 serum. pHRPGFPm2 (MRA-69) was provided by K. Haldar through MR4. A. G. was supported through the scholarship Kh149 from the Ministry of Higher Education and Scientific Research, Egyptian government. This work was supported in part by Grants-in-Aid for Scientific Research 16390126 (to M. T.) and 17590372 (to O. K.) from the Ministry of Education, Culture, Sports, Science and Technology, Japan.

References

[1] Bannister LH, Mitchell GH, Butcher GA, Dennis ED. Lamellar membranes associated with rhoptries in erythrocytic merozoites of *Plasmodium knowlesi*: a clue to the mechanism of invasion. Parasitology 1986;92:291–303.

[2] Sam-Yellowe TY, Shio H, Perkins ME. Secretion of *Plasmodium falciparum* rhoptry protein into the plasma membrane of host erythrocytes. J Cell Biol 1988;106:1507–13.

[3] Bannister LH, Hopkins JM, Fowler RE, Krishna S, Mitchell GH. Ultrastructure of rhoptry development in *Plasmodium falciparum* erythrocytic schizonts. Parasitology 2000;121:273–87.
[4] Jaikaria NS, Rozario C, Ridley RG, Perkins ME. Biogenesis of rhoptry organelles in *Plasmodium falciparum*. Mol Biochem Parasitol 1993;57:269–79.
[5] Topolska AE, Lidgett A, Truman D, Fujioka H, Coppel RL. Characterization of a membrane-associated rhoptry protein of *Plasmodium falciparum*. J Biol Chem 2004;279:4648–56.
[6] Campbell GH, Miller LH, Hudson D, Franco EL, Andrysiak PM. Monoclonal antibody characterization of *Plasmodium falciparum* antigens. Am J Trop Med Hyg 1984;33:1051–4.
[7] Holder AA, Freeman RR, Uni S, Aikawa M. Isolation of a *Plasmodium falciparum* rhoptry protein. Mol Biochem Parasitol 1985;14:293–303.
[8] Cooper JA, Ingram LT, Bushell GR, Fardoulys CA, Stenzel D, Schofield L, et al. The 140/130/105 kilodalton protein complex in the rhoptries of *Plasmodium falciparum* consists of discrete polypeptides. Mol Biochem Parasitol 1988;29:251–60.
[9] Hienne R, Ricard G, Fusaï T, Fujioka H, Pradines B, Aikawa M, et al. *Plasmodium yoelii*: identification of rhoptry proteins using monoclonal antibodies. Exp Parasitol 1998;90:230–5.
[10] Kaneko O, Tsuboi T, Ling IT, Howell S, Shirano M, Tachibana M, et al. The high molecular mass rhoptry protein, RhopH1, is coded by members of the *clag* multigene family in *Plasmodium falciparum* and *Plasmodium yoelii*. Mol Biochem Parasitol 2001;118:223–31.
[11] Ling IT, Florens L, Dluzewski AR, Kaneko O, Grainger M, Yim Lim BYS, et al. The *Plasmodium falciparum clag9* gene encodes a rhoptry protein that is transferred to the host erythrocyte upon invasion. Mol Microbiol 2004;52:107–18.
[12] Kaneko O, Yim Lim BYS, Iriko H, Ling IT, Otsuki H, Grainger M, et al. Apical expression of three RhopH1/Clag proteins as components of the *Plasmodium falciparum* RhopH complex. Mol Biochem Parasitol 2005;143:20–8.
[13] Ling IT, Kaneko O, Narum DL, Tsuboi T, Howell S, Taylor HM, et al. Characterisation of the *rhoph2* gene of *Plasmodium falciparum* and *Plasmodium yoelii*. Mol Biochem Parasitol 2003;127:47–57.
[14] Sam-Yellowe TY. Molecular factors responsible for host cell recognition and invasion in *Plasmodium falciparum*. J Protozool 1992;39:181–9.
[15] Rungruang T, Kaneko O, Murakami Y, Tsuboi T, Hamamoto H, Akimitsu N, et al. Erythrocyte surface glycosylphosphatidyl inositol anchored receptor for the malaria parasite. Mol Biochem Parasitol 2005;140:13–21.
[16] Lanzer M, Wickert H, Krohne G, Vincensini L, Braun-Breton C. Maurer's clefts: a novel multi-functional organelle in the cytoplasm of *Plasmodium falciparum*-infected erythrocytes. Int J Parasitol 2006;36:23–36.
[17] Vincensini L, Richert S, Blisnick T, Van Dorsselaer A, Leize-Wagner E, Rabilloud T, et al. Proteomic analysis identifies novel proteins of the Maurer's clefts, a secretory compartment delivering *Plasmodium falciparum* proteins to the surface of its host cell. Mol Cell Proteomics 2005;4:582–93.
[18] Waller RF, Reed MB, Cowman AF, McFadden GI. Protein trafficking to the plastid of *Plasmodium falciparum* is via the secretory pathway. EMBO J 2000;19:1794–802.
[19] Wickham ME, Rug M, Ralph SA, Klonis N, McFadden GI, Tilley L, et al. Trafficking and assembly of the cytoadherence complex in *Plasmodium falciparum*-infected human erythrocytes. EMBO J 2001;20:5636–49.
[20] Cheresh P, Harrison T, Fujioka H, Haldar K. Targeting the malarial plastid via the parasitophorous vacuole. J Biol Chem 2002;277:16265–77.
[21] Adisa A, Rug M, Klonis N, Foley M, Cowman AF, Tilley L. The signal sequence of exported protein-1 directs the green fluorescent protein to the parasitophorous vacuole of transfected malaria parasites. J Biol Chem 2003;278:6532–42.
[22] Marti M, Good RT, Rug M, Knuepfer E, Cowman AF. Targeting malaria virulence and remodeling proteins to the host erythrocyte. Science 2004;306:1930–3.
[23] Hiller NL, Bhattacharjee S, van Ooij C, Liolios K, Harrison T, Lopez-Estrano C, et al. A host-targeting signal in virulence proteins reveals a secretome in malarial infection. Science 2004;306:1934–7.
[24] Reed MB, Saliba KJ, Caruana SR, Kirk K, Cowman AF. Pgh1 modulates sensitivity and resistance to multiple antimalarials in *Plasmodium falciparum*. Nature 2000;403:906–9.
[25] VanWye JD, Haldar K. Expression of green fluorescent protein in *Plasmodium falciparum*. Mol Biochem Parasitol 1997;87:225–9.
[26] Trager W, Jensen JB. Human malaria parasites in continuous culture. Science 1976;193:673–5.
[27] Deitsch K, Driskill C, Wellems T. Transformation of malaria parasites by the spontaneous uptake and expression of DNA from human erythrocytes. Nucleic Acids Res 2001;29:850–3.
[28] Staalsoe T, Giha HA, Dodoo D, Theander TG, Hviid L. Detection of antibodies to variant antigens on *Plasmodium falciparum*-infected erythrocytes by flow cytometry. Cytometry 1999;35:329–36.
[29] Taylor HM, Grainger M, Holder AA. Variation in the expression of a *Plasmodium falciparum* protein family implicated in erythrocyte invasion. Infect Immun 2002;70:5779–89.
[30] Kaneko O, Fidock DA, Schwartz OM, Miller LH. Disruption of the C-terminal region of EBA-175 in the Dd2/Nm clone of *Plasmodium falciparum* does not affect erythrocyte invasion. Mol Biochem Parasitol 2000;110:135–46.
[31] Foth BJ, Ralph SA, Tonkin CJ, Struck NS, Fraunholz M, Roos DS, et al. Dissecting apicoplast targeting in the malaria parasite *Plasmodium falciparum*. Science 2003;299:705–8.
[32] Rug M, Wickham ME, Foley M, Cowman AF, Tilley L. Correct promoter control is needed for trafficking of the ring-infected erythrocyte surface antigen to the host cytosol in transfected malaria parasites. Infect Immun 2004;72:6095–105.
[33] Kocken CH, van der Wel AM, Dubbeld MA, Narum DL, van de Rijke FM, van Gemert GJ, et al. Precise timing of expression of a *Plasmodium falciparum*-derived transgene in *Plasmodium berghei* is a critical determinant of subsequent subcellular localization. J Biol Chem 1998;273:15119–24.
[34] Schatz G, Dobberstein B. Common principles of protein translocation across membranes. Science 1996;271:1519–26.
[35] Walter P, Johnson AE. Signal sequence recognition and protein targeting to the endoplasmic reticulum membrane. Annu Rev Cell Biol 1994;10:87–119.
[36] Treeck M, Struck NS, Haase S, Langer C, Herrmann S, Healer J, et al. A conserved region in the EBL proteins is implicated in microneme targeting of the malaria parasite *Plasmodium falciparum*. J Biol Chem 2006;281:31995–2003.
[37] Striepen B, Soldati D, Garcia-Reguet N, Dubremetz J, Roos D. Targeting of soluble proteins to the rhoptries and micronemes in *Toxoplasma gondii*. Mol Biochem Parasitol 2001;113:45–53.
[38] Hoppe HC, Ngo HM, Yang M, Joiner KA. Targeting to rhoptry organelles of *Toxoplasma gondii* involves evolutionarily conserved mechanisms. Nat Cell Biol 2000;2:449–56.
[39] Bradley PJ, Li N, Boothroyd JC. A GFP-based motif-trap reveals a novel mechanism of targeting for the *Toxoplasma* ROP4 protein. Mol Biochem Parasitol 2004;137:111–20.
[40] Wild J, Altman E, Yura T, Gross CA. DnaK and DnaJ heat shock proteins participate in protein export in *Escherichia coli*. Genes Dev 1992;6:1165–72.
[41] Rudiger S, Germeroth L, Schneider-Mergener J, Bukau B. Substrate specificity of the DnaK chaperone determined by screening cellulose-bound peptide libraries. EMBO J 1997;16:1501–7.
[42] Sanders SJ, Whiffield KM, Vogel JP, Rose MD, Schekman RW. Sec61p and BiP directly facilitate polypeptide translocation into the ER. Cell 1992;69:353–65.
[43] Brodsky JL, Schekman R. A Sec63p–BiP complex from yeast is required for protein translocation in a reconstituted proteoliposome. J Cell Biol 1993;123:1355–63.
[44] Panzner S, Dreier L, Hartmann E, Kostka S, Rapoport TA. Posttranslational protein transport in yeast reconstituted with a purified complex of Sec proteins and Kar2p. Cell 1995;81:561–70.
[45] Neupert W, Brunner M. The protein import motor of mitochondria. Nat Rev Mol Cell Biol 2002;3:555–65.
[46] Przyborski JM, Miller SK, Pfahler JM, Henrich PP, Rohrbach P, Crabb BS, et al. Trafficking of STEVOR to the Maurer's clefts in *Plasmodium falciparum*-infected erythrocytes. EMBO J 2005;24:2306–17.
[47] Sargeant TJ, Marti M, Caler E, Carlton JM, Simpson K, Speed TP, et al. Lineage-specific expansion of proteins exported to erythrocytes in malaria parasites. Genome Biol 2006;7:R12.

[48] Sam-Yellowe TY, Fujioka H, Aikawa M, Hall T, Drazba JA. A *Plasmodium falciparum* protein located in Maurer's clefts underneath knobs and protein localization in association with Rhop-3 and SERA in the intracellular network of infected erythrocytes. Parasitol Res 2001;87:173–85.

[49] Bradley PJ, Ward C, Cheng SJ, Alexander DL, Coller S, Coombs GH, et al. Proteomic analysis of rhoptry organelles reveals many novel constituents for host–parasite interactions in *Toxoplasma gondii*. J Biol Chem 2005;280:34245–58.

[50] Alexander DL, Mital J, Ward GE, Bradley P, Boothroyd JC. Identification of the moving junction complex of *Toxoplasma gondii*: a collaboration between distinct secretory organelles. PLoS Pathog 2005;1:137–49.

In vitro Antimalarial Activity of Flavonoids and Chalcones

Soon Sung Lim,† Hye-Sook Kim,‡ and Dong-Ung Lee*

*Department of Biotechnology, Dongguk University, Gyeongju 780-714, Korea. *E-mail: dulee@dongguk.ac.kr*
†Regional Innovation Center, Hallym University, Chunchon 200-702, Korea
‡Faculty of Pharmaceutical Sciences, Okayama University, Okayama 700-8530, Japan
Received August 16, 2007

Key Words : Flavonoids, Chalcones, Antimalarial activity, Cytotoxicity

Malaria is one of the most common infectious diseases in tropical and subtropical countries, including parts of the Americas, Asia, and Africa. Each year, it affects nearly 400-900 million people and causes approximately one to three million deaths annually.[1] Human malaria is caused by *Plasmodium falciparum*, *P. malariae*, *P. ovale*, and *P. vivax*, however, *P. falciparum* is the most prevalent for the disease and it is responsible for about 80% of infections and 90% of deaths.[2] The first effective treatment (17th century) against the *P. falciparum* parasite was the bark of cinchona tree, which contains quinine, a quinoline alkaloid. A number of medicines have been developed to treat malaria with chloroquine and its derivatives[3] as the mainstay therapy. In recent years, *P. falciparum* has become increasingly resistant to conventional antimalarial drugs, and the search for new antimalarial compounds by combining natural sources and synthetic approaches is still underway.[4,5]

As a part of our search[6-13] for novel antimalarial agents from plants or via chemical synthesis, we prepared twenty derivatives of flavonoids and chalcones. Flavonoids comprise a large group of polyphenolic secondary metabolites in plants. They are based on the flavan skeleton, consisting of two aromatic rings (ring A and B) interconnected by a three-carbon-atom, heterocyclic C ring, and classified into six main groups, flavanones, flavones, isoflavones, flavonols, flavanols, and anthocyanins. Many natural and synthetic flavonoids possess antimalarial activity.[14-17] Chalcones have a diverse array of substituents on the two aromatic rings of 1,3-diphenyl-2-propen-1-one, which was derived by the cleavage of the C ring in flavonoids. Depending on the substitution pattern on the two aromatic rings, chalcones have a wide range of biological activities, including antimalarial activity.[18-21] However, there has not been a direct comparison of flavonoids and chalcones and their structure-activity relationships.

In the present study, four derivatives for each of flavones (**1-4**), flavanones (**5-8**), chalcones (**9-12**), dihydrochalcones (**13-16**), and 3'-chloro-chalcones (**17-20**) (Fig. 1) were synthesized and evaluated for *in vitro* antimalarial activity against *P. falciparum* strain FCR-3 and cytotoxicity against FM3A cells (a mouse mammary tumor cell). The aim of this paper is to derive predictive structure-activity relationships to guide lead compound design.

Among the flavonoids and the related chalcones tested, the most active compounds were 3'-methyl-substituted flavanones (**5**) and 4'-methoxy-substituted dihydrochalcones (**15**), showing 100% inhibition against *P. falciparum* at the final concentration of 5.0 μg/mL and 5.4 μg/mL, respectively (EC_{50} = 1.6 μg/mL and 1.0 μg/mL, respectively) (Table 1). These compounds also showed strong cytotoxicity against FM3A cells, a model of the host, with relatively low EC_{50} values (>4.8 μg/mL and 3.3 μg/mL, respectively) and low selectivity indices (>3 and 3.3, respectively), indicating that these compounds have non-selective antimalarial activity. The selective toxicity index of quinine, a well-known antimalarial drug, was 450 in our previous report.[10] Eight compounds were weakly antimalarial, ten compounds were not cytotoxic, and five compounds showed no activity, but without cytotoxicity.

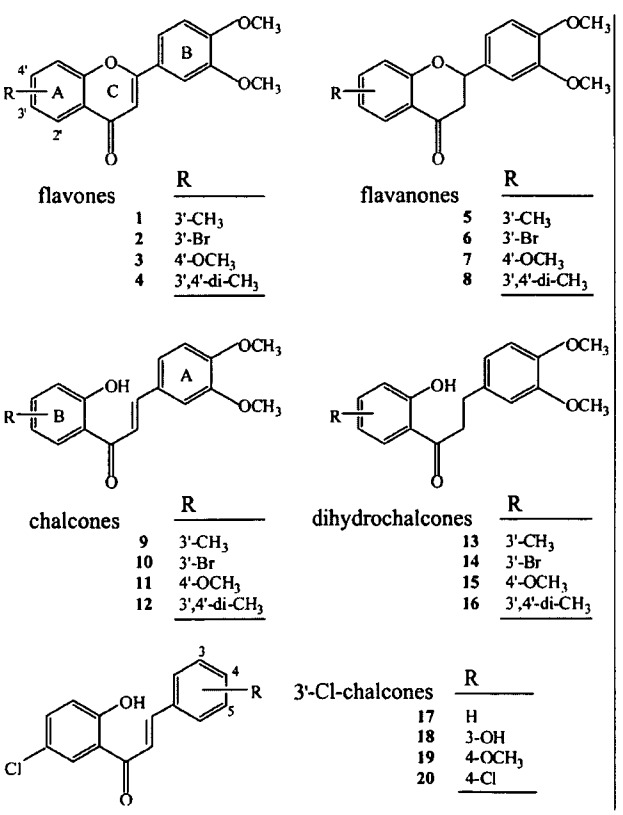

Figure 1. Chemical Structures of Tested Compounds.

Table 1. *In vitro* Antimalarial Activity and Cytotoxicity of tested compounds

Compound	Final Conc. (μg/mL)	*P. falciparum* % Inhibition (EC_{50})	FM3A EC_{50} (μg/mL)	Selectivity Index[a]
1	5.2	NA	NC	–
2	5.3	40	NC	–
3	5.8	37	3.2	–
4	5.2	13	2.0	–
5	5.0	100 (1.6)[b]	>4.8	>3
6	5.3	NA	NC	–
7	5.7	36	NC	–
8	5.2	NA	NC	–
9	5.4	NA	NC	–
10	5.2	22	1.7	–
11	5.4	37	1.4	–
12	5.5	5	NC	–
13	5.2	15	NC	–
14	5.1	NA	NC	–
15	5.4	100 (1.0)[b]	3.3	3.3
16	5.4	29	NC	–
17	5.2	14	1.7	–
18	5.0	NA	1.6	–
19	5.2	1	1.9	–
20	5.3	NA	2.8	–

[a]Selectivity index refers to the ratio of the EC_{50} value for the FM3A cells and the EC_{50} value for *P. falciparum*. [b]Values in parenthesis represent the EC_{50} value (μg/mL). NA = not active. NC = no cytotoxicity.

Antimalarial activity and cytotoxicity of the test compounds were influenced either by the kind or position of the substituents, or by the molecular skeleton. First, C-4'-methoxy substituents (**3**, **7**, **11**, **15**) were effective against *P. falciparum*, showing 36-100% inhibition at a concentration range of 5.4-5.8 μg/mL, and most C-3'-substitutions (**1**, **2**, **5**, **6**, **9**, **10**, **13**, **14**) had weak or no antimalarial activity, except compound **2** (40% inhibition) and **5** (100% inhibition, EC_{50} = 1.6 μg/mL). An α,β-unsaturated carbonyl structure (flavones **1-4** and chalcones **9-12**) increased the activity when the electron withdrawing or donating group was introduced at the C-3' or C-4' position. However, since the 3'-chloro-chalcones (**17-20**) were practically inactive, the substitution pattern in other aromatic rings may also affect antimalarial activity. Displacement of two methyl groups in compounds **4**, **12**, and **16** slightly elevated the activity compared to one methyl substitution (**1**, **9**, **13**) except **5**. Since the potent antimalarial activity of licochalcone A, a natural chalcone, was first reported,[22] over 200 chalcone derivatives have been assayed and their structure-activity relationships proposed,[19,22] but these studies did not include our novel synthetic chalcones.

In the cytotoxicity test, C-3'-chloro-substituted chalcones (**17-20**) with practically no antimalarial activity exhibited potent cytotoxicity against FM3A tumor cells (EC_{50} = 1.6-2.8 μg/mL). Together with the record of compound **10**, the chalcone compounds bearing a halogen group at C-3' with substituents in ring A were potent cytotoxic agents.

The introduction of other electron withdrawing or donating groups at C-4' in dihydrochalcones, as well as long-chain electron donating groups at C-3' in flavanones, would be useful for identifying other antimalarial agent.

Experimental Section

Materials. The flavonoid and chalcone derivatives used in this study were >98% pure and were synthesized according to methods described in our previous reports.[23,24] RPMI 1640 culture medium and fetal bovine serum were provided by Gibco (NY, U.S.A), and ES medium was purchased from Nissui Pharmaceuticals (Tokyo, Japan). Giemsa staining reagent was obtained from Merck (Germany). All other chemicals and reagents were of the highest grade available.

Malaria Parasites. *Plasmodium falciparum* (ATCC 30932, FCR-3 strain) was used in this study. *P. falciparum* was cultivated by a modification of the method of Trager and Jensen[25] using a 5% hematocrit of type A human red blood cells suspended in RPMI 1640 medium, and supplemented with heat-activated 10% type A human serum. The plates were placed in a CO_2-O_2-N_2 incubator (5% CO_2, 5% O_2 and 90% N_2 atmosphere) at 37 °C, and the medium was changed daily until 5% parasitemia (which means the existence of 5 parasite-infected erythrocytes in every 100 erythrocytes).

Mammalian Cells. Mouse mammary tumor FM3A cells (wild-type, subclone F28-7)[26] were supplied by the Japanese Cancer Research Resources Bank (JCRB). FM3A cells were maintained in a suspension culture at 37 °C in a 5% CO_2 atmosphere in plastic bottles containing ES medium supplemented with 2% heat-inactivated fetal bovine serum.

***In vitro* Antimalarial Activity Assay.** The following procedures were used to assay antimalarial activity.[12,13] Asynchronously cultivated *P. falciparum* was used. Various concentrations of compounds in DMSO were prepared. Five microliters of each solution was added to the individual wells of a 24-well multi-dish.

Erythrocytes with 0.3% parasitemia were added to each well containing 995 μL of culture medium to give a final hematocrit level of 3%. The plates were incubated at 37 °C for 72 h in a multigas incubator (5% CO_2, 5% O_2 and 90% N_2 atmosphere). To evaluate the antimalarial activity of the test compound, we prepared thin blood films from each culture and stained them with Giemsa. A total of 10000 erythrocytes per thin blood film were examined by microscopy. All of the test compounds were assayed in duplicate at each final concentration (5.0-5.8 μg/mL). Drug-free control cultures were run simultaneously. All data points represent the mean of three experiments. Parasitemia in the control reached between 4% and 5% at 72 h. The EC_{50} value refers to the concentration of the compound necessary to inhibit the increase in parasite density at 72 h by 50% of the control.

Toxicity against a Mammalian Cell Line. FM3A cells grew with a doubling time of about 12 h. Prior to drug exposure, cell density was adjusted to 5 × 10^4 cells/mL. A cell suspension of 995 μL was dispensed to the test plate,

and the compound at various concentrations suspended in DMSO (5 μL) was added to individual wells in a 24-well plate. The plates were incubated at 37 °C in a 5% CO_2 atmosphere for 48 h. All of the test compounds were assayed in duplicate at each concentration. Cell numbers were measured using a micro cell counter CC-130 (Toa Medical Electric Co., Japan). All data points represent the mean of three experiments. The EC_{50} value refers to the concentration of the compound necessary to inhibit by 50% the increase in cell density of the control at 48 h. Selectivity refers to the mean EC_{50} value for FM3A cells divided by the mean EC_{50} value for *P. falciparum*.

References

1. Breman, J. *Am. J. Trop. Med. Hyg.* **2001**, *64*, 1.
2. Mendis, K.; Sina, B.; Marchesini, P.; Carter, R. *Am. J. Trop. Med. Hyg.* **2001**, *64*, 97.
3. Wataya, Y.; Kim, H.-S. *Jikken Igaku* **2005**, *23*, 2741.
4. Gessler, M. C.; Nkunya, M. H. H.; Mwasumbi, L. B.; Heinrick, M.; Tanner, M. *ACTA Tropica* **1994**, *56*, 65.
5. Tran, Q. L.; Tezuka, Y.; Ueda, J.-Y.; Nguyen, N. T.; Maruyama, Y.; Begum, K.; Kim, H.-S.; Wataya, Y.; Tran, Q. K.; Kadota, S. *J. Ethnopharmacol.* **2003**, *86*, 249.
6. Iwasa, K.; Nishiyama, Y.; Ichimaru, M.; Moriyasu, M.; Kim, H.-S.; Wataya, Y.; Yamori, T.; Takashi, T.; Lee, D.-U. *Eur. J. Med. Chem.* **1999**, *34*, 1077.
7. Fujimoto, K.; Morisaki, D.; Yoshida, M.; Namba, T.; Kim, H.-S.; Wataya, Y.; Kourai, H.; Kakuta, H.; Sasaki, K. *Bioorg. Med. Chem. Letters* **2006**, *16*, 2758.
8. Kumura, N.; Izumi, M.; Nakajima, S.; Shimizu, S.; Kim, H.-S.; Wataya, Y.; Baba, N. *Bioscience, Biotechnology, and Biochemistry* **2005**, *69*, 2250.
9. Kim, H.-S.; Begum, K.; Ogura, N.; Wataya, Y.; Nonami, Y.; Ito, T.; Masuyama, A.; Nojima, M.; McCullough, K. J. *J. Med. Chem.* **2003**, *46*, 1957.
10. Takahara, M.; Kusano, A.; Shibano, M.; Kusano, G.; Koizumi, K.; Suzuki, R.; Kim, H.-S.; Wataya, Y. *Biol. Pharm. Bull.* **1998**, *21*, 823.
11. Kim, H.-S.; Nagai, Y.; Ono, K.; Begum, K.; Wataya, Y.; Hamada, Y.; Tsuchiya, K.; Masuyama, A.; Nojima, M.; McCullough, K. *J. Med. Chem.* **2001**, *44*, 2357.
12. Kim, H.-S.; Shibata, Y.; Wataya, Y.; Tsuchiya, K.; Masuyama, A.; Nojima, M. *J. Med. Chem.* **1999**, *42*, 2604.
13. Kim, H.-S.; Miyake, H.; Arai, M.; Wataya, Y. *Parasitology International* **1998**, *47*, 59.
14. Kanokmedhakul, S.; Kanokmedhakul, K.; Nambuddee, K.; Kongsaeree, P. *J. Nat. Prod.* **2004**, *67*, 968.
15. Beldjoudi, N.; Mambu, L.; Labaieed, M.; Grellier, P.; Ramanitrahasimbola, D.; Rasoanaivo, P.; Martin, M. T.; Frappier, F. *J. Nat. Prod.* **2003**, *66*, 1447.
16. Auffret, G.; Labaied, M.; Frappier, F.; Rasoanaivo, P.; Grellier, P.; Lewin, G. *Bioorg. Med. Chem. Letters* **2007**, *17*, 959.
17. Tasdemir, D.; Lack, G.; Brun, R.; Ruedi, P.; Scapozza, L.; Perozzo, R. *J. Med. Chem.* **2006**, *49*, 3345.
18. Li, R.; Chen, X.; Gong, B.; Dominguez, J. N.; Davidson, E.; Kurzban, G.; Miller, R. E.; Nuzum, E. O.; Rosenthal, P. J. *J. Med. Chem.* **1995**, *38*, 5031.
19. Valla, A.; Valla, B.; Cartier, D.; Le Guillou, R.; Labia, R.; Florent, L.; Charneau, S.; Schrevel, J.; Potier, P. *Eur. J. Med. Chem.* **2006**, *41*, 142.
20. Narender, T. S.; Tanvir, K.; Srinivasa Rao, M.; Srivastava, K.; Puri, S. K. *Bioorg. Med. Chem. Letters* **2005**, *15*, 2453.
21. Liu, M.; Wilairat, P.; Go, M.-L. *J. Med. Chem.* **2001**, *44*, 4443.
22. Chen, M.; Theander, T. G.; Christensen, B. S.; Hviid, L.; Zhai, L.; Kharazmi, A. *Antimicrob. Agents Chemother.* **1994**, *38*, 1470.
23. Lim, S.-S.; Jung, S.-H.; Ji, J.; Shin, K.-H.; Keum, S.-R. *Chem. Pharm. Bull.* **2000**, *48*, 1786.
24. Lim, S.-S.; Jung, S.-H.; Ji, J.; Shin, K.-H.; Keum, S.-R. *J. Pharm. Pharmacol.* **2001**, *53*, 653.
25. Trager, W.; Jensen, J. B. *Science* **1976**, *193*, 673.
26. Yoshioka, A.; Tanaka, S.; Hiraoka, O.; Koyama, Y.; Hirota, Y.; Ayusawa, D.; Seno, T.; Garrett, C.; Wataya, Y. *J. Biol. Chem.* **1987**, *262*, 8235.

Preparation of Quinoline Hexose Analogs as Novel Chloroquine-Resistant Malaria Treatments (1). Synthesis of 4-Hydroxyquinoline-β-glucosides

Hiroshi SUZUKI,*[a] Nagwa S. M. ALY,[b] Yusuke WATAYA,[b] Hye-Sook KIM,[b] Ikumi TAMAI,[c] Masaki KITA,[d] and Daisuke UEMURA[e]

[a] *National Research Center for Protozoan Diseases, Obihiro University of Agriculture and Veterinary Medicine; Inada-cho, Obihiro, Hokkaido 080–0555, Japan:* [b] *Faculty of Pharmaceutical Sciences, Okayama University; 1–1–1 Tsushima Naka, Okayama, Okayama 700–8530, Japan:* [c] *Faculty of Pharmaceutical Sciences, Tokyo University of Science; 2641 Yamasaki, Noda, Chiba 278–8510, Japan:* [d] *Research Center for Materials Science, Nagoya University; and* [e] *Department of Chemistry, Graduate School of Sciences, Nagoya University; Chikusa-ku, Nagoya, Aichi 464–8602, Japan.*

Received December 23, 2006; accepted February 19, 2007; published online February 22, 2007

Quinoline hexose analogs are expected to be useful as novel agents for treatment of chloroquine-resistant malaria. Here, we report preparation of 4-hydroxy quinoline-β-glucosides from anilines in 4 steps.

Key words malaria; chloroquine-resistant malaria treatment; quinoline-glucosides

Malaria is one of the most serious infectious diseases in the developing world, with mortality estimated at *ca.* 2.5 million deaths annually, mainly caused by the erythrocytic-stage cells of *Plasmodium falciparum*.[1] For four decades, malaria has been treated effectively with the 4-aminoquinoline analog chloroquine (CQ). However, CQ-resistant strains of *Plasmodium* spp. have spread and continue to evolve.[1] Therefore, the development of new chemotherapeutic agents that are effective against CQ-resistant malaria is required.

Malaria parasites are known to take up hemoglobin in their food vacuole as a source of amino acids and release ferriprotoporphyrin IX (FP IX) into the food vacuole and cytoplasm in the erythrocytic stage.[2] FP IX is very toxic to *Plasmodium* spp., which explains why they have detoxification systems to deal with this complex.[2] The parasite's food vacuole is acidic, and so CQ accumulates in the vacuole due to its basic quinoline moiety.[2] CQ is thought to inhibit detoxification of FP IX in the food vacuole by forming a complex between the quinolinic nitrogen of CQ and Fe(II) of FP IX.[2] Various mechanisms have been proposed to explain CQ resistance, but none have been proven conclusively.[3] All of the proposed mechanisms of CQ resistance have several points in common: (1) the concentration of CQ in the food vacuole of CQ-resistant strains is lower than that in CQ-sensitive strains, and (2) CQ-resistance is reversible because CQ-resistant strains can recover CQ sensitivity under some conditions.[3] In this context, quinoline analogs that can be concentrated in the cytoplasm of malaria parasites may be suitable as novel chemotherapeutic candidates against CQ-resistant malaria because they would facilitate maintenance of a high concentration of quinoline in the food vacuole by osmosis, and the detoxification of FP IX in the cytoplasm can be inhibited.

Metabolism and transport of carbohydrates are essential for cell viability. Carbohydrates are transported into the cell through hexose transporters (HTPs), which are membrane proteins expressed on the cell surface.[4] Furthermore, HTPs transport hexose analogs, such as glycosides.[5] These molecules can be utilized as novel drug delivery systems (DDS) that can act as carriers and import medicines efficiently into the cell through HTPs.

Malaria parasites have a high demand for carbohydrates in the erythrocytic stage and often cause hypoglycemia.[6] Accordingly, quinoline hexose analogs can be expected to concentrate quinolines into the cytoplasm of the malaria parasite by the above DDS and serve as novel chemotherapeutic candidates for treatment of CQ-resistant malaria. Here, we report the synthesis of quinoline-β-glucosides in a systematic preparation of quinoline hexose analogs.

Results and Discussion

The target compounds **5a**—**f** were prepared from the corresponding anilines (**1a**—**f**) in 4 steps shown in Charts 1, 2, 3, and 4.

As shown in Chart 1, 4-hydroxyquinoline-3-ethylesters **2a**—**f** were prepared from the corresponding anilines **1a**—**f** by a modification of the method of Price and co-workers[7] in the yields shown.

Hydrolysis of **2a**—**f** with 2 N-sodium hydroxide at room temperature for 2 h afforded the corresponding crude quinoline carbonic acids, which were then heated in diphenylether under reflux. The decarboxylation described above gave compounds **3a**—**f** in the yields shown in Chart 2.

The quinoline ring is generally sensitive to reductive conditions. The benzyl group is considered unsuitable as a protecting group in quinoline glucosides, because the deprotection reaction requires reductive conditions. Therefore, the acetyl group was adopted for protection of the hydroxyl group of D-glucose. 1-Bromo-tetraacetyl-α-D-glucose was prepared from pentaacetyl-D-glucose and 30%-hydrobromic acid in acetic acid solution.[8] The reaction conditions were determined by using 4-hydroxyquinoline (**3g**) and 7-chloro-4-hydoxyquinoline (**3h**), both of which were commercial

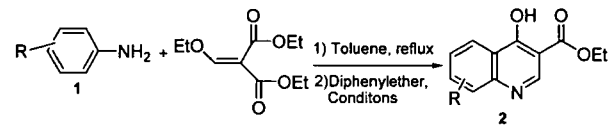

1 2

		Conditions	Yield (%)
1a R=4-Me-	**1a** R=6-Me-	reflux, 1 h	45
1b R=4-MeO-	**1b** R=6-MeO-	reflux, 1 h	36
1c R=3-MeO-	**1c** R=7-MeO-	230°C, 12 h	14
1d R=4-PhO-	**1d** R=6-PhO-	reflux, 1 h	30
1e R=4-Me_2N-	**1e** R=6-Me_2N-	reflux, 1 h	67
1f R=4-PhNH-	**1f** R=6-PhNH-	reflux, 2 h	35

Chart 1

* To whom correspondence should be addressed. e-mail: hiroshis@obihiro.ac.jp